Aus dem Institut für Physiologie
der Medizinischen Fakultät Charité Berlin-Universitätsmedizin
Campus Benjamin Franklin

DISSERTATION

Effects of Vertigoheel® on the Microcirculation of Spontaneously Hypertensive Rats

zur Erlangung des akademischen Grades
Doctor medicinae (Dr. med.)

vorgelegt der Medizinischen Fakultät
Charité – Universitätsmedizin Berlin

von

Lasti Erfinanda

aus Pekanbaru

Datum der Promotion: 01.03.2019

Dedication

This dissertation is dedicated to the very precious people that I have in my life. To my loving parents Fuaadi Ibrahim and Ernani Fuaadi, and to my brothers and sister, Pinto Fernanda, Reno Kanti Riananda, and Ferdi Endinanda: thank you for always be there to support me.

Table of Contents

Zusammenfassung

Ziel: In früheren Studien wurde die Effektivität von Vertigoheel® gegen Schwindel belegt. Diese Erkrankung geht mit einer beeinträchtigten mikrovaskulären Perfusion des vertebrobasilaren Systems im Bereich des Innenohrs einher. Darüber hinaus wurde eine vasorelaxierende Wirkung von Vertigoheel® gezeigt, welche im Zusammenhang mit der synergistischen Stimulation der zyklischen Nukleotid-Signalwege steht. Daraus erwächst die Annahme, dass Vertigoheel® einen positiven Effekt auf weitere Krankheiten wie vaskuläre Demenz (VaD) haben könnte, die mit einer beeinträchtigten mikrovaskulären Perfusion und/oder Dysfunktion der Gefäßwand assoziiert sind. In dieser Arbeit wird die Hypothese aufgestellt, dass Vertigoheel® eine vasorelaxierende Wirkung auf die zerebrale Mikrozirkulation bei spontan hypertensiven Ratten (SHR) hat. Das Ziel dieser Arbeit war die Bestätigung der vasorelaxierenden Wirkung von Vertigoheel® auf die zerebrale Mikrozirkulation von SHR, sowie die Bestimmung der daran möglicherweise beteiligten Mechanismen.

Methoden: Die mikrovaskuläre Reaktivität der Haut auf Acetylcholin (ACh) und Natrium-Nitroprussid (SNP) wurde mittels Laser-Doppler-Flowmetrie (LDF) in der Rückenhaut von 16 Wochen alten SHR und Wistar Kyoto Ratten (WKY) bestimmt. Anschließend wurde je eine Gruppe von SHR und WKY Ratten mit Vertigoheel® intraperitoneal (2 ml • kg-1 • d-1) dreimal pro Woche über acht Wochen behandelt, Je eine Gruppe von SHR und WKY Ratten diente als unbehandelte Kontrolle. Nach acht Wochen wurde die mikrovaskuläre Reaktivität der Haut erneut bestimmt, gefolgt von einer zerebralen mikrovaskulären LDF-Antwort auf moderate Hyperkapnie (5% CO_2). Die Expression der endothelialen Stickoxidsynthase (eNOS), der Phosphodiesterase 5 (PDE5) und der Phosphodiesterase 4 (PDE4) im zerebralen Gewebe wurde mittels Western Blotting ermittelt. Die zerebrale Konzentration von zyklischem Adenosinmonophosphat (cAMP) und zyklischem Guanosinmonophosphat (cGMP) wurde mittels ELISA gemessen.

Ergebnisse: Die primäre Beurteilung der mikrovaskulären Reaktivität der Haut zeigte Relaxationsstörungen bei SHR im Vergleich zu WKY Ratten sowohl nach ACh und SNP Applikation. Nach achtwöchiger Verabreichung von Vertigoheel® ergab die mikrovaskuläre Reaktivitätsneubewertung keinen Unterschied zwischen der SHR-Vertigoheel-Gruppe (SHR-V) und der SHR-Kontrollgruppe (SHR-C). Die Differenz in der mikrovaskulären Reaktivität zwischen SHR und WKY konnte nicht mehr nachgewiesen werden. Die zerebrale mikrovaskuläre Antwort auf Hyperknapie dagegen fiel bei SHR-V signifikant höher aus als bei SHR-C. Es zeigte sich kein signifikanter Unterschied zwischen der Wistar Kyoto- Vertigoheel®-

Gruppe (WKY-V) und der Wistar Kyoto-Kontrollgruppe (WKY-C). In den Western-Blots ergab sich eine signifikant höhere eNOS-Expression bei SHR-V als bei SHR-C Tieren. Es wurde kein Unterschied zwischen WKY-V und WKY-C beobachtet. Es wurden keine Unterschiede in der PDE5 oder PDE4 Expression und in den Gewebekonzentrationen von cAMP oder cGMP bei SHR-V im Vergleich zu SHR-C Ratten oder zwischen WKY-V und WKY-C Tieren nachgewiesen.

Schlussfolgerung: Vertigoheel® hat eine vasorelaxierende Wirkung auf die zerebrale Mikrozirkulation von SHR-V nach einer Applikationsdauer von acht Wochen. Dieser Effekt könnte mit einer gesteigerten Expression der eNOS assoziiert sein.

Abstract

Objective: Earlier studies have demonstrated that Vertigoheel® increased perfusion in a skin area considered as proxy to the inner ear of vertigo patients. Furthermore, the vasorelaxant effect has been shown to be related to the synergistic stimulation of cyclic nucleotide signalling pathways. We speculated that Vertigoheel® might provide a beneficial effect for further diseases that are associated with impaired microvascular perfusion and/or dysfunction of the vessel wall, such as vascular dementia (VaD). In this study we hypothesized that Vertigoheel® would have a vasorelaxant effect on cerebral microcirculation in spontaneously hypertensive rats (SHR). Therefore, the aim of this study was to investigate whether Vertigoheel® has a vasorelaxant effect on the cerebral microcirculation of SHR and to assess the putative mechanisms of this effect.

Methods: Baseline skin microvascular vasodilatory responses to acetylcholine (ACh) and sodium nitroprusside (SNP) were assessed with laser-Doppler flowmetry (LDF) in the dorsal skin of 16-week-old SHR and Wistar Kyoto rats (WKY). Vertigoheel® was administered intraperitoneally (2 ml • kg^{-1} • d^{-1}), three times per week for 8 weeks. After 8 weeks, skin microvascular reactivity was reassessed, followed by LDF cerebral microvascular assessment of the perfusion response to mild hypercapnia (5% CO_2). Expressions of endothelial nitric oxide synthase (eNOS), phosphodiesterase 5 (PDE5), and phosphodiesterase 4 (PDE4) in cerebral tissue were assessd using Western blotting. Cerebral cyclic adenosine monophosphate (cAMP) and cyclic guanosine monophosphate (cGMP) tissue concentrations were measured with ELISA.

Results: Baseline skin microvascular reactivity assessment showed relaxation disturbance in SHR compared to WKY in response to both, ACh and SNP. After 8 weeks of Vertigoheel® administration, skin microvascular reactivity reassessment showed no difference between SHR Vertigoheel® treatment (SHR-V) and the SHR control group (SHR-C). The baseline vasorelaxation difference between SHR and WKY was not found any more in the second assessment of skin microvascular reactivity. However, the cerebral microvascular response was significantly greater in SHR-V than SHR-C. No significant difference between Wistar Kyoto Vertigoheel® treatment (WKY-V) and Wistar Kyoto control group (WKY-C) was detected. Western blotting result showed significantly higher eNOS expression in the SHR-V than in the SHR-C. No such difference was observed between the WKY-V and WKY-C. No differences were detected in PDE5 and PDE4 expression, cAMP, or cGMP in SHR-V compared with SHR-C, nor in WKY-V compared with WKY-C.

Conclusion: Vertigoheel® has a vasorelaxant effect on the cerebral microcirculation of SHR-V after 8 weeks administration. This effect might be associated with increased eNOS expression in SHR cerebral tissue.

List of Figures

List of Tables

Abbreviations

ACh: Acetylcholine

AD: Alzheimer's dementia

BBB: Blood-brain barrier

cAMP: Cyclic adenosine monophosphate

CBF: Cerebral blood flow

CMVR: Cerebral microvascular reactivity

cGMP: Cyclic guanosine monophosphate

CNS: Central nervous system

CSF: Cerebrospinal fluid

ELISA: Enzyme-linked immunosorbent assay

eNOS: Endothelial nitric oxide synthase

LDF: Laser-Doppler flowmetry

MAP: Mean arterial pressure

MDA: Malonaldehyde

NO: Nitric oxide

PDE4: Phosphodiesterase 4

PDE5: Phosphodiesterase 5

SHR: Spontaneously hypertensive rats

SHR-C: Spontaneously hypertensive rats control group

SHR-V: Spontaneously hypertensive rats Vertigoheel® treated group

SNP: Sodium nitroprusside

SVD: Small-vessel disease

VaD: Vascular dementia

WKY: Wistar-Kyoto rats

WKY-C: Wistar-Kyoto rats control group

WKY-V: Wistar-Kyoto rats Vertigoheel® treated group

1 Introduction

Improvements in health care, health knowledge, nutrition, and hygiene lead to increased life expectancy (1). Accordingly, data from the United Nations shows that the elderly population is increasing in developed and developing countries (2). Based on these data, the number of people aged >65 years old will increase from 600 million to 2 billion, and the number of people over the age of 80 will increase from 105 million to 400 million (2). The increased prevalence of older people in the population increases the incidence of non-communicable diseases (2).

Dementia, a syndrome characterized by progressive deterioration of cognitive functions, is one of these non-communicable diseases and one of the main causes of disability in the elderly (3). The global incidence of dementia is appraised to be 35.6 million people in 2010 (4). Due to the increasing elderly population, it is predicted that the total number of patients with dementia worldwide will double every 20 years. It will be 65.7 million people in 2030 and 115.4 million people in 2050 (4). The total cost of dementia worldwide is estimated at 604 million US $ in 2010 (4) and is estimated to increase markedly with the expected higher number of dementia patients in the future. Furthermore, behavioral and psychological changes due to dementia not only directly impact the patients but also affect the medical, psychological, and emotional wellbeing of the family and the caregivers. (5).

Vascular dementia (VaD) is the second most common form of dementia in the elderly after Alzheimer's disease (AD). Yet, with the prediction of a higher incidence of stroke in the near future (6), one of the risk factors for VaD, it is possible that VaD will become the most common form of dementia in the elderly (7). Despite being one of the main causes of disability in the elderly and has severe impact on individuals' lives and society in general, the treatment options for and research on VaD are still very limited and there are no effective approved pharmacological treatments available for VaD (8). The use of anti-platelet and anticoagulant drugs that are usually used for stroke treatment show unsatisfying results and also have major side effects such as major bleeding (9;10). Anti-hypertension drugs have been shown to inhibit the progression of VaD in the elderly. However, the use of anti-hypertension medication in patients with normal blood pressure could cause excessive hypotension leading to cerebral infarction (11;12). Cholinesterase inhibitors and memantine, drugs that modulate neurotransmission abnormality, produced only small benefits in VaD (13) and the effect size of the drug is limited (14). Thus, it can be concluded that further innovations in therapy for VaD are required.

The pathogenesis of VaD involves disturbance of the cerebral microvasculature. Disturbances in the microvasculature contribute to the formation of white matter lesions in cerebral tissue (15). One of the risk factors that can cause microangiopathy in cerebral tissue is hypertension. Epidemiological studies have consistently shown that hypertension, diabetes, obesity, hypercholesterolemia, smoking, and lack of physical activity increase the risk of dementia and cognitive impairment (16). Hypertension in mid-life can increase the risk for VaD at older age (17). Continuous exposure to high blood pressure has been shown to damage the cerebral microvasculature (18). Exposure of the cerebral microvasculature to high blood pressure can also lead to lipohyalinosis and vascular remodelling, which may induce luminal narrowing in the arteries and arterioles that penetrate into cerebral white matter. Due to the primary functions of the microvasculature to optimize the supply of oxygen and nutrient to the tissues and to keep constant hydrostatic pressure in the capillary vessels, this can lead to damage of the white matter and of cortical connections (7) Based on this pathogenetic relationship between the microcirculation and VaD the microvasculature may be a therapeutic target for prevention or treatment of VaD.

Vertigoheel® is a low dose combination preparation that is commonly used to treat vertigo. In a clinical double-blinded, controlled study for vertigo related to atherosclerosis, Vertigoheel® has been shown to have the same effect as *Ginkgo biloba*, the standard drug for vertigo in Europe (19). One of the causes of vertigo is microvascular perfusion disturbance in the inner ear (20). An intravital microscopy study in vestibular vertigo patients has shown that Vertigoheel® can improve the microcirculation in a skin area behind the ear lobe regarded as proxy to the inner ear (21). A study from Heinle et al demonstrated that Vertigoheel® has a vasorelaxing effect in the isolated rat carotid artery. Another observation in this study was that the mechanism of Vertigoheel® might involve the synergistic effects from cyclic nucleotide pathways in vascular smooth muscle cells. Additionally, Vertigoheel® also increased the production of nitric oxide (NO) (22). It can be concluded from these findings that Vertigoheel® has a potential effect of microvascular vasodilation.

Taken together, protective effects of Vertigoheel® on the microcirculation could be applied not only to treat vertigo, but also to other diseases related to disturbances of microvascular perfusion or to vascular dysfunction, such as in VaD. In this study we tested the effect of Vertigoheel® in Spontaneously Hypertensive Rats (SHR) which has been shown to have microvascular dysfunction. The SHR also have cerebrovascular disturbance characteristics similar to those in hypertensive humans. In SHR, reductions in the external diameter and increases in the media-to-lumen ratio of cerebral arterioles have been reported (23). Blood

pressure increasing with age, brain hypotrophy, loss of neuronal cells, and glial reactions are some phenomena that occur in brains of hypertensive patients that also occur in SHR (24). This study hypothesizes that Vertigoheel® may improve cerebral microvascular perfusion in SHR. The aims of this study are to investigate whether Vertigoheel® will increase cerebral microvascular perfusion in SHR and to determine the underlying mechanisms of this improved microvascular function.

2 Literature Review

2.1 Vascular Dementia

Vascular dementia (VaD) is a loss of cognitive function that has effects on activities of daily live. It is caused by cerebrovascular disease due to ischemia or haemorrhage, cardiovascular disease, or circulatory disturbances that affect the brain regions responsible for memory, cognition, or behaviour (25). The risk factors for VaD are divided into four major groups: demographic, atherosclerotic, genetic, and stroke-related. Demographic risk factors include age, male sex, and lower educational level. The major atherosclerotic risk factors are a history of hypertension, cigarette smoking, myocardial infarction, diabetes mellitus, and hyperlipidemia. The genetic risk factors include familial vascular encephalopathies such as cerebral autosomal dominant arteriopathy with subcortical infarct and leukoencephalopathy (CADASIL). The stroke-related risk factors are the volume of cerebral tissue loss, evidence of bilateral cerebral infarction, strategic infarction, and white-matter disease (26).

Pathologically, there are two causes of VaD. The first involves disturbances in large or medium vessels, and the second disturbances in small vessels. The most common cause of VaD is a disturbance in the cerebral microcirculation (cerebral small vessel disease (SVD)) (27). Disturbances in small vessels can cause lesions in the white-matter which are related to focal cerebral ischemia (28). From a study using arterial spin-labelling magnetic resonance imaging, damage in sub cortical vessels was related to decrease cerebral blood flow (CBF) to the cortex (29). Hypertension is the number one risk factor for SVD and is a leading cause of cognitive decline and dementia (30). Chronic hypertension in middle age can produce cognitive impairment through its effects on the microvasculature and subsequent ischemic and anatomic damage (31). Hypertension will cause lipohyalinosis and vascular remodelling, which will decrease cerebral perfusion (28;30). Additionally, chronic hypertension can also reduce CBF by disturbing the mechanisms that regulate the CBF (30).

2.1.1 Pathophysiology of Vascular Dementia

Dysfunction of the neurovascular unit and mechanisms regulating cerebral blood flow are likely to be important components of the pathophysiological processes underlying VaD (32). This dysfunction is associated with disturbances in the cerebral microvasculature. Structural and functional changes in cerebral microvessels play a role in the disturbance of cerebral microvasculature (33). In VaD, the cerebral microvessels undergo basal membrane thickening,

become tortuous or twisted, and show rarefaction (34). Another study has also shown that arteriole wall structure in VaD presents like an onion skin due to hyaline degeneration (lipohyalinosis) (33). This structural change will lead to narrow lumina and occlusion in small arteries, arterioles, and capillaries that go deep into the white matter. The stenosis of these vessels will impair tissue perfusion and cause acute or chronic ischemia. The impact of acute and chronic ischemia in the brain is damage of the neurovascular unit that could blunt the functional hyperaemia response (30).

One of the causes of the damage in the neurovascular unit is increased permeability of the blood-brain barrier (BBB). The changes in brain microvasculature in response to chronic hypertension, such as lipohyalinosis and fibrosis, will lead to ischemia that may induce BBB failure, which further contributes to lacunar strokes and dementia. One study has shown that chronic hypertension induced alteration of the BBB by modulating the protein expression level (35). Alterations of the BBB will cause increased BBB permeability or even BBB failure that will lead to neurovascular unit damage (36). Leakage of fluid and macromolecules from the microvessels can cause cerebral perivascular inflammation and demyelination of axons in the white-matter which will ultimately slow the saltatory neuronal conduction (32). Another study also proposed that endothelial injuries will produce BBB leakage, leading to vessel ruptures and microbleeding, which will finally result in cystic infarction of the surrounding parenchyma (37).

Both the structural changes and increased permeability of cerebral microvessels occur because of cerebral endothelial dysfunction as the underlying mechanism. Endothelium, after the discovery of nitric oxide (NO), turned out to be a major regulator in blood vessels including cerebral vessels (38). In normal endothelial function, NO plays a crucial role in maintaining vascular homeostasis, including modulation of vascular dilator tone. It also has anti-atherosclerotic properties, such as regulation of local cell growth, and protection of the vessel from injurious consequences of platelets and leukocytes circulating in the blood (39). Hypertension causes vascular remodelling in the entire systemic vasculature including the cerebral vessels. Chronic hypertension is associated with adaptive and degenerative structural changes in cerebral resistance vessels and plays a major role in endothelial dysfunction (31). In recent years, it has become apparent that hypertension can increase vascular oxidative stress. Increased vascular oxidative stress will lead to endothelial dysfunction. The result of increased oxidative stress is a decrease in NO bioavailability and uncoupling of the eNOS resulting in production of reactive oxygen species (ROS) instead of NO. ROS can sequester NO by forming peroxynitrite, a very potent radical species, thus reducing circulating NO. Oxidation of tetrahydrobiopterin (BH4) leads to the uncoupling of eNOS from NO production and

subsequently superoxide can be formed (40). Endothelial dysfunction induced by vascular oxidative stress can induce the release of vascular endothelial growth factor and prostanoids, which promote vascular leakage, protein extravasation, and cytokine production (32). Oxidative stress is also correlated with VaD. Several studies found that oxidative stress status is altered in VaD. Alterations of oxidative stress status in VaD were shown as reduced vitamin C levels in plasma, reduced α-tocopherol, increased malonaldehyde (MDA), and increased oxidative DNA damage repair in cerebrospinal fluid (CSF) and urine (41). These microvascular changes caused by hypertension occurred systemically. Skin microcirculation changes can be detected non-invasively using Laser Doppler Flowmetry (LDF). One such study showed that disturbance in skin microcirculation correlates with the occurrence of VaD (42)

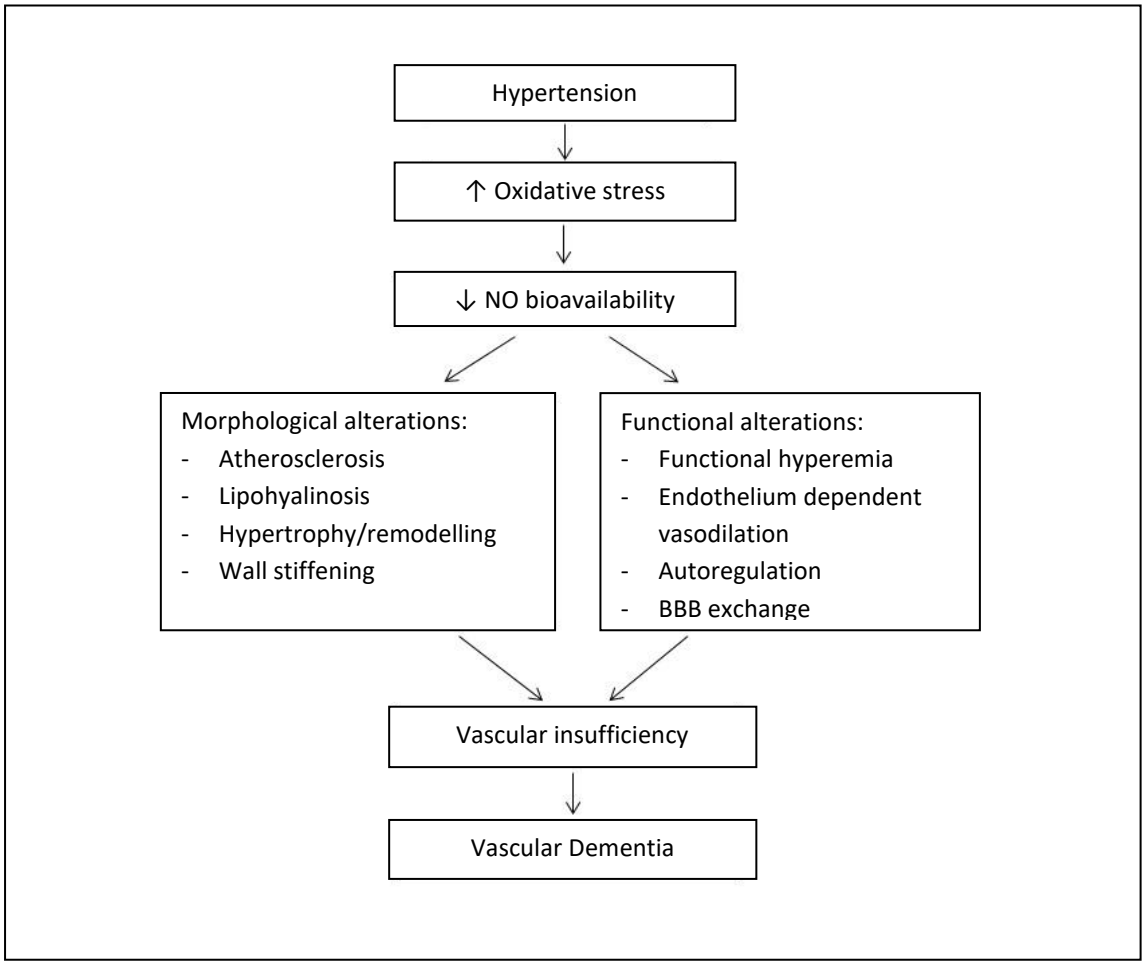

Fig. 1: Schematic diagram of VaD pathophysiology. Modified from Iadecola C., et al. (30;32)

2.2 Microcirculation

The microcirculation, based on anatomical definition, includes blood vessels with diameters <150 μm. According to this definition the microcirculation will cover the arterioles,

capillaries, and venules. Physiologically, the microcirculation is defined to include all the vessels in which the lumen diameter decreases or the vascular smooth muscle constricts in response to an increase in blood pressure (23).

Functionally, the microvascular bed can be divided into resistance, exchange, and capacitance vessels (43):

Resistance vessels (Small Arteries and Arterioles): The diameters of resistance vessels range from 10-200 μm. Arterioles form the final branch of arterial systems and mark the beginning of the microcirculation. Arterioles present with a large number of smooth muscle cells to control vascular resistance in the microcirculation.

Exchange vessels (Capillaries): The diameter of capillaries is 5-9 μm. Capillaries consist of a single layer of endothelium and no smooth muscle cells but occasional pericytes. The structure is optimized to maintain their primary function as exchange vessels.

Capacitance vessels (Venules): The diameter of venules is greater than 10 μm and with increasing size they start to acquire smooth muscle cells. Venules belong to the capacitance vessels which hold 70% of the total circulating blood volume and, due to their high compliance, can easily adapt to blood volume changes.

Hence, in addition to their tasks of fulfilling nutritional and oxygen demand in tissues, the microcirculation also plays a crucial role in determining total peripheral resistance and in blood pressure regulation (23).

2.2.1 Anatomy of Cerebral Circulation

The brain is an organ that requires continuous perfusion. A disturbance in cerebral perfusion may lead to dysfunction or even death (32). A complicated cerebrovascular control mechanism is required to maintain CBF supply to meet the brain's demand (44). Blood supply to the brain comes from two internal carotid arteries and two vertebral arteries. The internal carotid arteries branch to form two major cerebral arteries, the anterior and middle cerebral arteries. The right and left vertebral arteries form the midline basilar artery. The basilar artery anastomoses with the arteries from the internal carotids in an arterial ring at the base of the brain (in the vicinity of the hypothalamus and cerebral peduncles) called the circle of Willis. The posterior cerebral arteries arise at this confluence, as do two small bridging arteries: the anterior and posterior communicating arteries. From the base of the brain, these arteries branch into the leptomeningeal or pial arteries. The pial artery branches perpendicularly to the brain parenchyma into penetrating intracerebral arteries and arterioles (20-90 μm diameters in the human brain).

The penetrating arteries branch into the arterioles and capillaries. The diameter of these latter vessels is 6-10 μm in the human brain (45). The arterial vessels in the brain are comprised of three layers, the tunica intima (endothelium and sub-endothelial tissue), the tunica media (vascular smooth muscle cells), and the tunica adventitia (connective tissue with collagen, fibroblasts, neurons, and vasa vasorum) (46)

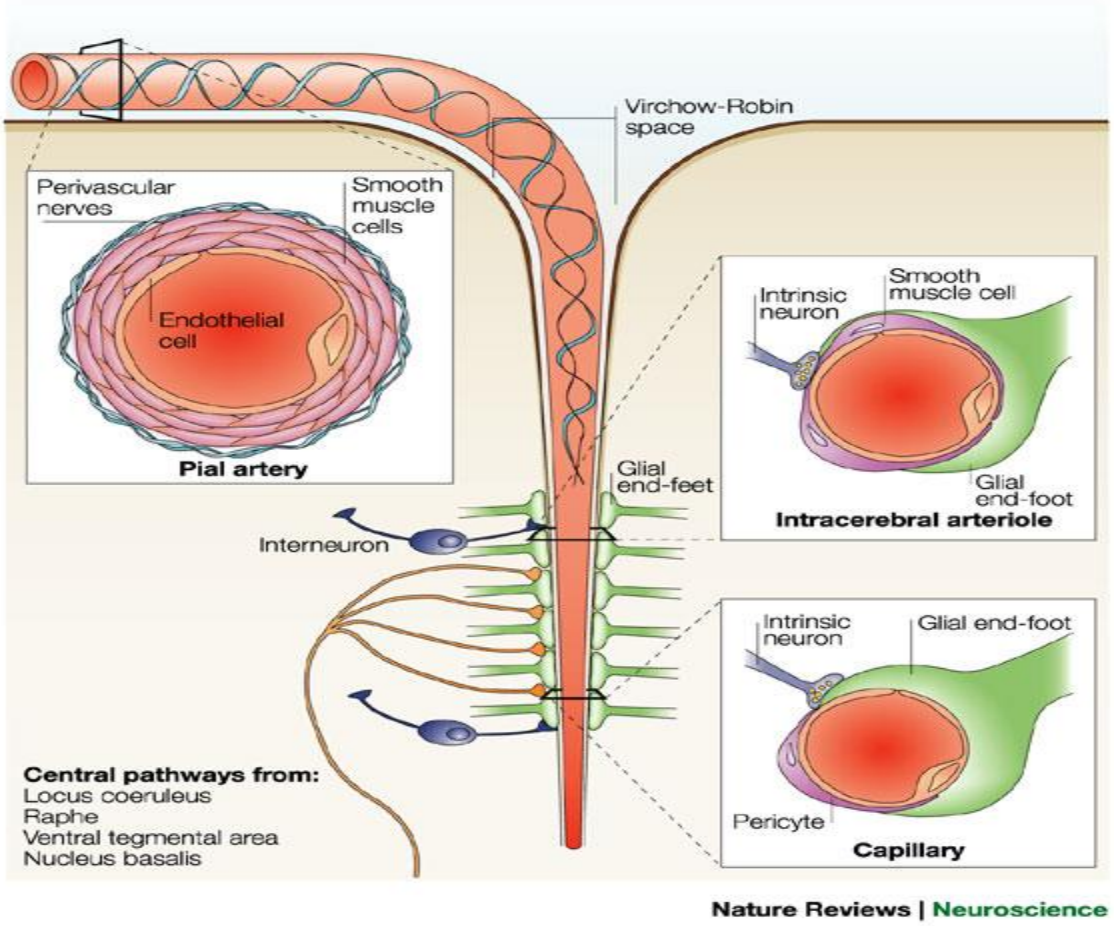

Fig. 2: Structure of the brain with vasculature and the neurovascular unit (according to Iadecola C., et al) (47)

2.2.2 Cerebral Microcirculation Physiology

2.2.2.1 Neurovascular Unit

The physiological balance in the cerebral micro-environment is coordinated by the neurovascular unit. The neurovascular unit is comprised of monolayered endothelial cells, integral neighboring cells, and foot processes from astrocytes that cover the vascular wall and neuronal terminals (32). The function of the neurovascular unit is to control the exchange of molecules across the BBB, regulate CBF, contribute to cerebral immunity, and provide trophic support in brain cells (48)

2.2.2.2 Blood-Brain Barrier

Three cellular elements of the brain microvasculature compose the BBB: endothelial cells as the primary barrier, pericytes, and astrocyte end-feet (49). The process of molecular exchange in the microcirculation of the brain is stricter than in other parts of the body. This is caused by the structure of the endothelium in the brain, which is quite different from the endothelium in other parts of the body. The monolayered endothelium in the cerebral microcirculation is connected with tight junctions. These tight junctions will restrict the diffusion flow of charged molecules and water-soluble molecules across the BBB (50). The cerebral endothelium also contains selective specific transport barriers to select substances from crossing from the vascular lumen into the tissue (51). To protect the brain tissue, the BBB also contains a metabolic barrier that is run by a combination of extracellular and intracellular enzymes (52). Another difference is that the BBB contains fewer transport vesicles compared to other vessels in the human body (53). In performing their role, endothelial cells work together with basal lamina, pericytes, and astrocyte end-feet in the neurovascular unit. This collaboration regulates the permeability of the BBB (54).

2.2.2.3 Regulation of Cerebral Blood Flow

The regulation of CBF is maintained by the cerebral auto regulation, cerebral metabolic flow regulation, and cerebral neurogenic regulation. In the neurovascular unit, endothelium and astrocytes work together to achieve CBF regulation (55).

2.2.2.3.1 Cerebral Auto Regulation

The CBF is maintained at a constant flow even when the driving force for perfusion, the mean arterial pressure (MAP), changes. In healthy individuals the CBF remains rather constant between MAP values of 60 to 140 mmHg. This capability of the cerebral resistance vessels is defined as cerebral auto regulation (50;55). Cerebral auto regulation will shift to the right, to higher MAP values, in chronic hypertension. This condition is related to vascular remodelling and structural changes of the cerebral resistance vessel. Low blood pressure that would be tolerated by healthy individuals may cause ischemia in this situation (56).

The underlying mechanism of cerebral autoregulation is named myogenic control or Bayliss effect. Increased transmural pressure induces passive distension of the vessel wall which is sensed by vascular smooth muscle cells which respond by active constriction to diameters

below the baseline diameter prior to pressure increase. Thus vascular resistance increases to a degree that equalizes the increased blood pressure and perfusion remains unchanged (55). Another mechano-sensory mechanism of perfusion regulation is wall shear stress mediated regulation where increased perfusion induces dilation of resistance vessels (55). In bigger arterioles and small arteries, the neurogenic regulation through sympathetic perivascular nerves in the tunica adventitia contributes to the regulation of vessel diameters (57).

2.2.2.3.2 Metabolic Control

Increased activity from any part of the brain will increase the blood flow to that part. This phenomenon is called functional hyperemia or metabolic coupling of perfusion (45). There are some molecules that are under investigation and expected to mediate the relation between neuronal activity and regulation of CBF. The tissue concentration of these molecules increases with synaptic transmission, either because they are involved in the process itself, or because there production and release increase with increased cellular metabolism (50). The best investigated molecules and ions that contribute to metabolic control of perfusion include adenosine, hydrogen ions (H^+), potassium ions (K^+), and carbon dioxide (CO2). An increased tissue concentration of these molecules and ions will result in vasodilatation (50;55).

2.2.2.3.3 Neurogenic Control

Neurogenic regulation also plays a role in maintaining the CBF. There are two types of neural regulation: extrinsic and intrinsic. Extrinsic innervation refers to vessel innervation outside the brain parenchyma. The three main sources of perivascular innervation are the trigeminal ganglion for sensory, the superior cervical ganglion for sympathetic, and the sphenopalatine ganglion for parasympathetic innervation. The sympathetic nerves innervate the large cerebral vessels, and it has been hypothesized that the main role of the sympathetic nervous system is to increase tone, in order to maintain blood pressure below the upper limit of the autoregulatory mechanism. The parasympathetic system has been proposed to play a role in pathological states (50;55;57). After the blood vessels enter the brain parenchyma the innervation changes from extrinsic into intrinsic. In intrinsic pathways, the nerves are not attached directly to the microvessels, but instead they connect to astrocyte foot processes. The nucleus basalis, locus coeruleus, and raphe nucleus have all been described as a source of innervation of the cerebral microvasculature (55;58).

2.2.2.3.4 Endothelial Control

The endothelium makes a major contribution to the regulation of CBF. Endothelium in cerebral vessels, like other endothelia in other vessels in the body, bridges the communication between vessel lumen and vascular smooth muscle cells. Some vasoactive mediators that are produced by the endothelium are: nitric oxide (NO), endothelium-derived hyperpolarizing factor (EDHF), prostacyclin (PGI_2), prostaglandin (PGE_2), and endothelin (50;55). NO, EDHF, PGI_2, or PGE_2 can induce vasodilatation in cerebral vessels. On the other hand, vasoconstriction results from various mechanisms including decreased NO bioavailability or release of endothelin (30;50;55).

The endothelial cells play a role in maintaining the basal tone of the cerebral arteries and arterioles by constantly releasing NO (38). NO diffuses from the endothelium to the vascular smooth muscle cells, where it binds to and activates soluble guanylate cyclase (sGC). This enzyme converts guanosine triphosphate (GTP) into cyclic guanosine monophosphate (cGMP). Increased intracellular levels of cGMP will activate cGMP-dependent protein kinase (PKG). PKG mediates vascular smooth muscle relaxation by a number of mechanisms, including lowering of intracellular free Ca^{2+} levels and phosphorylation of myosin light chain phosphatase, desensitizing the contractile apparatus to Ca^{2+} (59). Phosphodiesterase (PDE) will control the development of smooth muscle relaxation by degrading cGMP. The phosphodiesterases that specifically hydrolyze cGMP are phosphodiesterase 5 (PDE5), 6 (PDE6), and 9 (PDE9). These PDEs will degrade cGMP by hydrolyzing cGMP into 5'-GMP (30;38;50;55).

Nitric oxide synthase (NOS) is the enzyme that catalyzes NO production from L-arginine and molecular oxygen. There are three isoforms of NOS, neuronal NOS (nNOS or NOS1), inducible NOS (iNOS or NOS2), and endothelial NOS (eNOS or NOS3). Under normal conditions, neurons express nNOS and cerebral vessels express eNOS. Neurons and cerebral vessels can express iNOS under pathological conditions such as hypertension or lipopolysaccharide exposure (60).

Although vasodilatation is the best known and most studied effect of endothelial NO, many other functions have been identified in studies on animals and *in vitro*. NO has been described to suppress platelet aggregation, leucocyte adhesion to the endothelium and emigration, to attenuate vascular smooth muscle cell proliferation and migration. Furthermore, NO can inhibit activation and expression of certain endothelial adhesion molecules, and influence production of superoxide anions. Loss of endothelium-derived NO would be expected to promote a vascular phenotype more prone to atherogenesis (38). Decreased NO activity is

related to an imbalance between ROS and the antioxidant scavenger system. An increase in ROS will decrease NO bioavailability (30;61).

A second important vasodilator produced by endothelial cells is prostacyclin (PGI_2). PGI_2 is a metabolite from arachidonic acid produced via the cyclooxygenase (COX) pathway. Arachidonic acid is metabolized to a number of products that are collectively called eicosanoids (62). Some eicosanoids are dilators while others are constrictors. The metabolic pathway of arachidonic acid starts with the liberation of arachidonic acid from the phospholipid membrane, primarily by phospholipase A2. After being liberated, arachidonic acid is metabolized by COX, lipoxygenase, epoxygenase, or Ω hydroxylase. Dilator products of the COX pathway include prostacyclin (PGI_2), prostaglandin E_2, and prostaglandin D_2. Constrictor products include prostaglandin $F_{2\alpha}$ and thromboxane A_2 (TXA_2). The release of PGI_2 by cerebral endothelial cells activates G-protein-coupled receptors on vascular smooth muscle cells which activate adenylyl cyclase. Adenylyl cyclase transforms adenosine triphosphate (ATP) into cyclic adenosine monophosphate (cAMP). The intracellular cAMP will activate cAMP-dependent protein kinase (PKA). Activation of PKA opens K^+ channels and causes hyperpolarization of the smooth muscle cell. Voltage-sensitive Ca^{2+} channels close, resulting in decreased intracellular Ca^{2+} concentration and vasodilatation (63). cAMP also has other functions beside relaxation of smooth muscle, such as inhibiting proliferation of smooth muscle cells. Once cAMP is generated, the only way to inactivate it is to degrade it to 5'-AMP, through phosphodiesterase (PDE) action. The PDE that specifically hydrolyzes cAMP is PDE 4 (30;38;50;55).

The third mechanism of endothelial cells that induces vasodilatation in cerebral micro-vessels is through EDHF. The hallmark of the EDHF pathway is insensitivity to agents that block the production of NO or PGI_2, but it is blocked by the combination of charybdotoxin and apamin. It has been shown that there is involvement of intermediate-conductance Ca^{2+}-activated K^+ channels (IK_{ca}) and small-conductance Ca^{2+}-activated K^+ channels (SK_{ca}). The term EDHF refers to a factor released by the endothelial cells. This factor involves the opening of a potassium channel. The release of EDHF requires an increase in endothelial intracellular calcium concentration which will open calcium activated potassium channels. Hyperpolarization of endothelial cells initiates the formation of EDHF, which is then transferred to the vascular smooth muscle cells (VSMC) via myoendothelial gap junctions or evokes the release of a hyperpolarizing factor that acts directly on smooth muscle cells (63).

Vasoconstriction of cerebral microvessels is mediated by endothelin. The endothelin system is composed of two receptors (ETA and ETB) and three ligands (ET-1, ET-2, and ET-3). ETA receptors are found predominantly in vascular smooth muscle cells, are stimulated by ET-1

and ET-2, and mediate vasoconstriction. ETB receptors are found predominantly within the endothelium, are stimulated by all three ligands, and mediate vasodilatation (50).

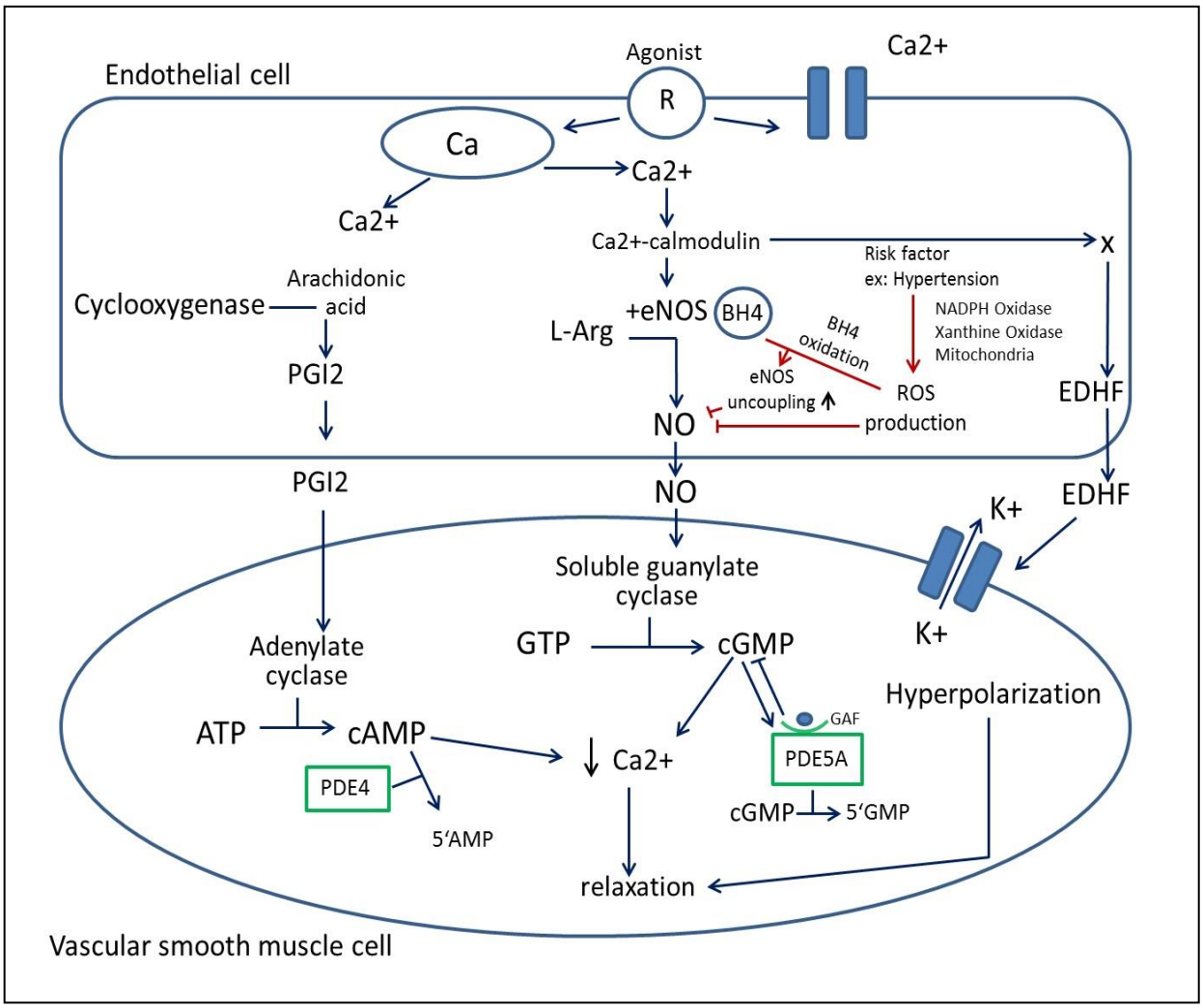

Fig. 3: Schematic diagram of vasodilatory mechanism (63-65)

2.3 Spontaneously Hypertensive Rats (SHR)

SHR are an animal model for essential or primary hypertension in humans. Like hypertension in humans, hypertension in SHR also occurs gradually with age and the cause is not known. SHR have normal blood pressure when they are born, and their blood pressure increases during age 2-4 months. At the age of 6 months, the hypertension in SHR already sustains. The development of the SHR strain was begun in the 1950s by Okamoto and colleagues by breeding male Wistar-Kyoto rats (WKY) with mild hypertension (systolic pressure 145-175 mmHg) with female WKY with relatively high blood pressure (systolic pressure 130-140 mmHg). After selecting offspring who were hypertensive by repeatedly checking their blood pressure, Okamoto

and colleagues were able to establish a colony of rats developing hypertension and reported them as SHR in 1963 (24). In experiments, usually normotensive WKY serve as controls for SHR (66).

Hypertension in SHR as well as in humans can also result in end-organ damage. Several studies have proposed that the cerebral changes in SHR are associated with vascular remodelling and endothelial dysfunction caused by hypertension (24;67;68). Peripheral resistance vessels in SHR as well as in hypertensive humans undergo vascular remodelling, that is structural changes in the vascular wall. These changes can be observed as narrowed lumen, decrease in number of microvessels, and greater malformation of the vessel (67). Reductions in the external diameter and increases in the media-to-lumen ratio of cerebral arterioles have been reported (23). An immunohistochemistry study on 12-weeks-old SHR found that the microvasculature in the cerebrum and striated muscle decreased in density ("rarefaction") (69). Additionally, another study also found that cerebral arterioles from SHR undergo eutrophy and hypertrophy on the inner side. Blood vessels in the frontal cortex of 24-week-old SHR showed wall hypertrophy and luminal narrowing (70).

2.4 Vertigoheel®

Vertigoheel® is a low dose combination preparation containing *Ambra grisea* D6, *Anamirta cocculus* D4, *Conium maculatum* D3, and petroleum rectificatum D8, whereby D6, D4, D3, and D8 denote the potentiation of the various ingredients of the homeopathic preparation (19). Vertigoheel® has long been available over-the-counter in several countries with an established record of general use for vertigo treatment (71). It has been demonstrated that Vertigoheel® has the same efficacy as *Ginkgo biloba*. *G. biloba* itself is already registered as a drug in Germany and several other European countries and has been shown to have a superior efficacy and good tolerability compared with placebo in studies of vestibular and nonvestibular vertigo. In a double-blind, randomized, controlled study, Vertigoheel® was shown to have the same efficacy as *Ginkgo biloba* in reducing the severity, duration, and frequency of vertigo. In this study, 170 patients, ages 60–80 years, with atherosclerosis-related vertigo received treatment with Vertigoheel® or *Ginkgo biloba*. The result showed that Vertigoheel® is not inferior to *Ginkgo biloba* in improving vertigo. This study also showed excellent tolerability for Vertigoheel® by patients (72). A meta-analysis has also confirmed that Vertigoheel® has an effectiveness equal to other established anti-vertiginous drugs (71).

Despite the popularity of Vertigoheel®, the exact mechanism of this drug has not been conclusively studied. One of the causes of vertigo is disturbance of the microvascular perfusion in the inner ear or vertebrobasilar system (73). Thus there is a possibility that the improvement of vertigo in the patients of the study just mentioned is due to Vertigoheel® enhancing microvascular perfusion. This hypothesis is supported by the intra-vital microscopy study in vertigo patients that demonstrated increased perfusion in skin regarded as proxy to the inner ear. After 12 weeks of treatment, patients treated with Vertigoheel® showed an increased number of nodal points, increased flow rate of erythrocytes in arterioles and venules, increased vasomotion, and a slight reduction in local hematocrit compared to baseline. These changes in Vertigoheel® treated patients were not observed in the control group and the differences between the treatment and control groups were statistically significant. The microcirculatory changes were associated with a reduction in the severity of vertigo in the treated patients, both as assessed by the treating physician and as reported by the patients themselves (21).

Based on the hypothesis that Vertigoheel® may exert beneficial vascular effects, Heinle et al. proposed that the vasorelaxant effect of Vertigoheel is produced by stimulating the adenylate and/-or guanylate cyclase pathways. In their *in vitro* study, they confirmed their hypothesis by demonstrating an inhibitory effect on PDE5 by *Conium maculatum*, one ingredient of Vertigoheel®. They also observed that increasing the dosage of *Anamirta cocculus* stimulated the activation of the adenylate cyclase. This effect was not seen with other ingredients of Vertigoheel®. Vertigoheel® also induced a significant vasorelaxant effect in isolated pre-contracted rat carotid arteries in a vessel myography experiment (22). This finding confirmed the previous study of Vertigoheel®, which had also demonstrated a vasodilatory effect of Vertigoheel® (21). Combining the findings from these studies one may conclude that Vertigoheel® could have the general potential to protect the microcirculation. This opens the possibility that Vertigoheel® could be used to treat other diseases, besides vertigo, that are also caused by perfusion disturbances.

3 Materials and Methods

3.1 Materials

3.1.1 Experimental Animals

Experiments were performed on 16 weeks old (body weight 350 ± 50 gr) SHR and WKY. They were obtained from Charles River (Charles River Laboratories, Research Models and Services GmbH, Freiburg, Germany). The animals were housed in standard cages in a temperature-controlled room (22-25°C) with a 12 h dark-light cycle. They received standard laboratory chow (Altromin, Lage, Germany) and water ad libitum.

All animals received care in accordance with the Guide for the Care and Use of Laboratory animals. All procedures and protocols for animal experiments had been approved by the respective local authorities (Berliner Landesamt für Gesundheit und Soziales, project number G0446/09).

3.1.2 Substances and Chemicals

Table 1: Overview of substances and suppliers for skin microvascular assessment

Substances	Dosage	Supplier
Acetylcholine	2%	Sigma-Aldrich, Taufkirchen, Germany
Sodium Nitroprusside	2%	Schwarz Pharma, Monheim am Rhein, Germany
Vertigoheel®	0.2 ml/kg	Biologische Heilmittel Heel GmbH, Baden-Baden, Germany

Buffers and chemical solutions for Western Blot

- Electrophoresis Buffer: Tris-Glycine SDS Buffer
- Immunoblotting Buffer: Tris-Glycine containing 20% methanol
- PBS Buffer: Phosphate-Buffered Saline containing NaCl 137 mM, KCl 2.7 mM, Na_2HPO_4 10 mM, KH_2PO_4 1.8 mM (pH 7.4).
- PBST Buffer: Phosphate-Buffered Saline containing NaCl 137 mM, KCl 2.7 mM, Na_2HPO_4 10 mM, KH_2PO_4 1.8 mM and 0.2% Tween 20.

- Laemmli Buffer: containing 4% SDS, 20% glycerol, 10% 2-mercaptoethanol, 0.004% bromphenol blue, in 0.125 M Tris HCl.
- Separating gel 8%: containing ProSieve 50 Gel solution (Lonza, Cologne, Germany) 3.2 ml, 1.5 M Tris-HCL ph 8.8 5 ml, 10% SDS Solution 0.2 ml, 10% Ammonium Persulfate (APS) (Sigma-Aldrich, Taufkirchen, Germany) 200 µl, Temed (Sigma-Aldrich, Taufkirchen, Germany) 8 µl.
- Collecting gel 5%: ProSieve 50 Gel solution 1 ml, 1 M Tris-HCL ph 6.8 1.3 ml, 10% SDS solution 100 µl, 10% APS 100 µl, and Temed 10 µl.
- Extraction Buffer: 1 tablette protease inhibitor cocktail (complete, Mini Protease Inhibitor Cocktail, Basel, Switzerland), PBS Dulbecco (Biochrom GmbH, Berlin, Germany) 9.4 ml, PMSF (Sigma.Aldrich, Taufkirchen, Germany) 100 µl, and Triton X (Sigma-Aldrich, Taufkirchen, Germany) 500 µl.
- peqGold Prestained Protein-Marker VII (Peqlab, Erlangen, Germany)

Antibodies

Table 2: Overview of antibodies for Immunoblotting

Primary Antibodies	Dilution	Secondary Antibodies	Supplier
Rabbit anti-rat eNOS	1:500	Goat anti-rabbit IgG	Santa Cruz Biotechnology, Dallas, Texas, United States
Rabbit anti-rat PDE5A	1:2000	Goat anti-rabbit IgG	Santa Cruz Biotechnology, Dallas, Texas, United States
Rabbit anti-rat PDE4	1:1000	Goat anti-rabbit IgG	Abcam Biotechnology, Cambridge, United Kingdom

ELISA

- Parameter cAMP assay kit KGE002B, R&D system, Minneapolis, Minnesota, United States
- Parameter cGMP assay kit KGE003, R&D system, Minneapolis, Minnesota, United States

Equipment

- Laser-Doppler Flowmetry Periflux PF3 from Perimed, Stockholm, Sweden
- Laser-Doppler Flowmetry probe 408 from Perimed, Stockholm, Sweden
- Laser-Doppler Flowmetry probe 308 from Perimed, Stockholm, Sweden
- Double-sided adhesive discs from 3M health care, Neuss, Germany
- Multitool Drill from Dremel 300 series, Breda, Netherland
- Micromanipulator
- Animal respirator advanced 4601-1 from TSE System GmbH, Bad Homburg, Germany
- Gas mixture 5% CO_2, 21% O_2, rest N_2 Linde, Munich, Germany
- Transducer BD DTX Plus™ from Becton Dickinson critical care system, Singapore
- Electrophoresis system Mini-PROTEAN® Tetra Cell for Mini Precast Gels from Bio-rad Laboratories GmbH, Munich, Germany
- Blotting system Trans-Blot® SD Semi-Dry Transfer Cell, Bio-rad Laboratories GmbH, Munich, Germany
- Homogenizer T10 basic Ultra Turrax, IKA GmbH, Staufen, Germany

3.2 Methods

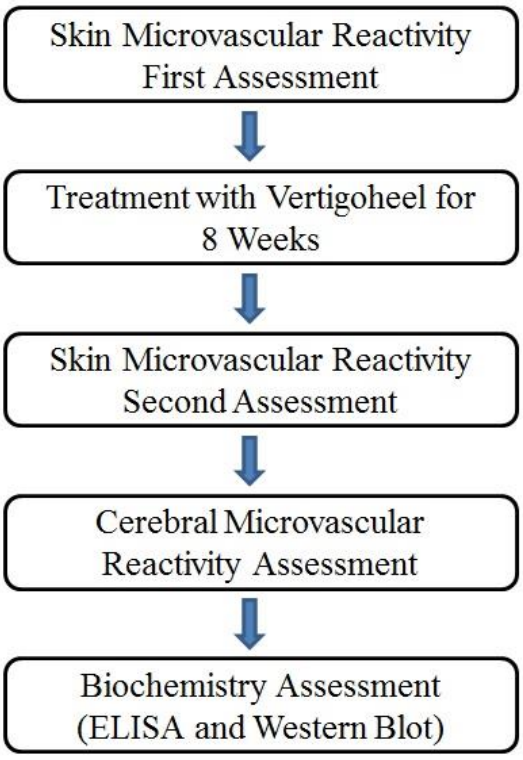

Fig. 4: The steps of the experimental procedure

3.2.1 Skin Microvascular Reactivity Assessment

Before the administration of Vertigoheel®, we assessed the skin microvascular function by measuring the cutaneous blood flow of the rats with laser-Doppler flowmetry (LDF) (Periflux PF3 Perimed, Stockholm, Sweden). To expose the skin, we shaved the hair from the back of the rats with an electric clipper (Moser, Unterkirnach, Germany) one day before the measurement. On the next day the animals were sedated with an intraperitoneal injection of Ketamine (0,12 ml/100gr) (Ketavet, Pharmacia GmbH, Erlangen, Germany) and Xylazine (0,06 ml/100gr) (Bayer Vital GmbH, Leverkusen, Germany) and placed in a prone position on a heating pad. Body temperature was always maintained at 37 ± 0.5°C. The LDF probe (LDF probe 408 Perimed, Stockholm, Sweden) was placed directly on the skin on the back of the rats. During positioning of the probe, areas with visible vessels were avoided and position was secured with adhesive tape (double-sided adhesive discs 3M Health Care, Neuss, Germany). As a baseline measurement, cutaneous blood flow was recorded for 5 minutes followed by 0.05 ml subcutaneous injection of 2% solutions of Acetylcholine (Sigma Aldrich, Taufkirchen, Germany) or Sodium Nitroprusside (Nipruss, Schwarz Pharma, Monheim am Rhein, Germany) with a 26 G needle (Braun Melsungen AG, Melsungen, Germany) exactly beneath the LDF probe. The cutaneous blood flow was recorded with Scope software (Scope version 2.2.0.30© 2000 Data Translation Inc, Bietiheim-Bissingen, Germany) until the peak or a plateau had been reached. We performed the cutaneous blood flow measurement with acetylcholine (ACh) as endothelium dependent vasodilator and sodium nitroprusside (SNP), an NO donor, as endothelium independent vasodilator. Each ACh or SNP measurement was performed using the same procedure on either the left or right side of the back. ACh or SNP were dissolved in saline 0.9% (Fresenius Kabi, Bad Homburg, Germany) to produce a 2% solution. Data was analyzed with Chart5 for Windows software (ADInstruments, Oxford, United Kingdom).

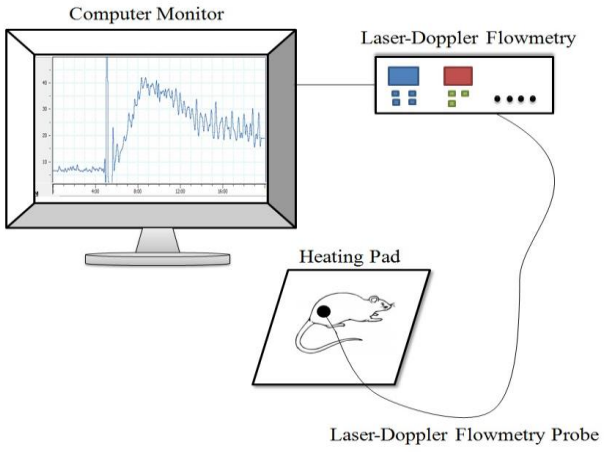

Fig. 5: Schematic diagram of the skin microvascular reactivity measurement

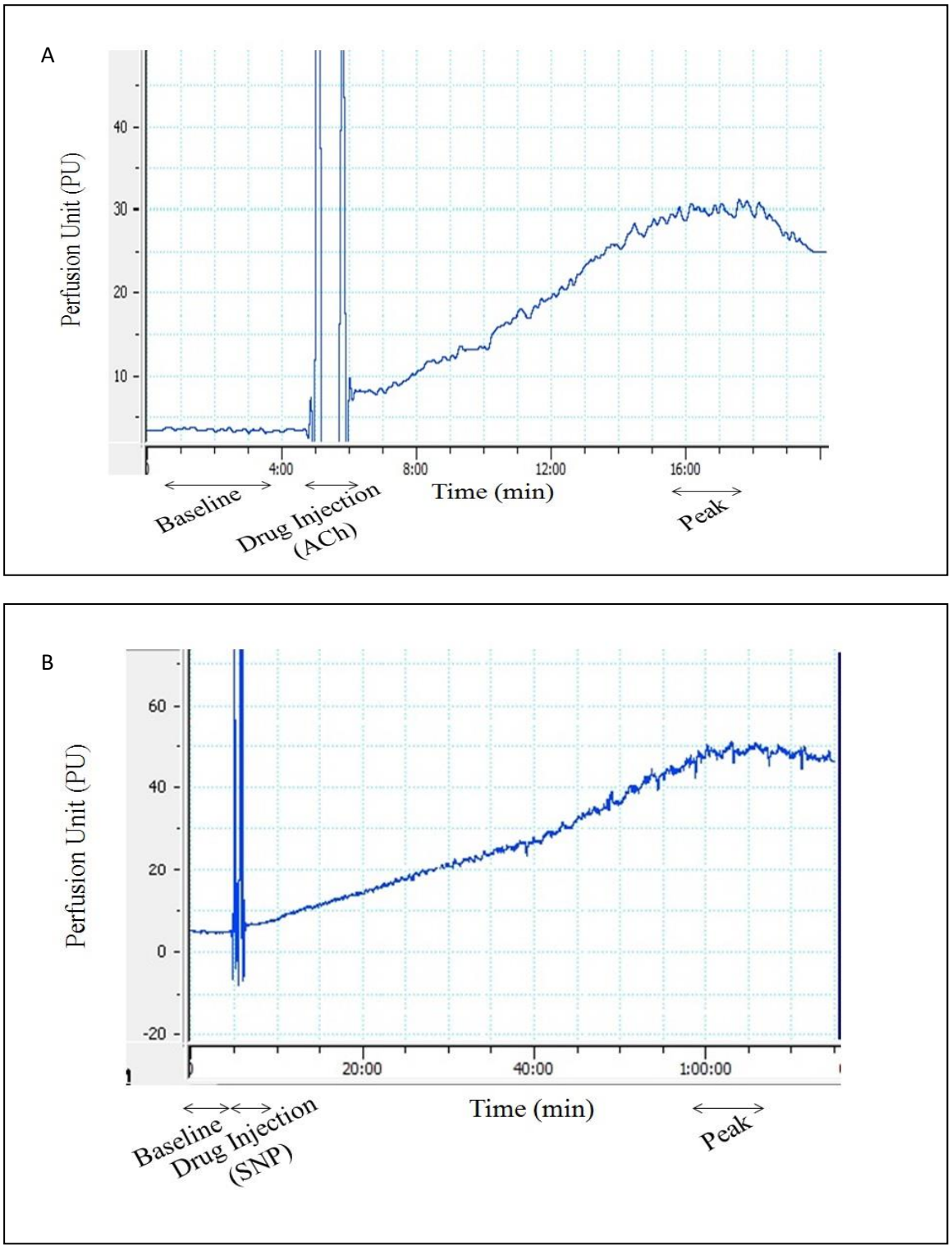

Fig. 6: Examples of skin microvascular reactivity assessment by stimulation with either ACh (A, top) or SNP (B, bottom). Skin perfusion was measured by LDF.

3.2.2 Vertigoheel® Administration

The animals were divided into 4 groups: SHR treated with Vertigoheel® **(**Biologische Heilmittel Heel GmbH, Baden-Baden, Germany) (SHR-V n=16), SHR as controls (SHR-C

n=15), WKY treated with Vertigoheel® (WKY-V n=16), and WKY as controls (WKY-C n=15). In the Vertigoheel® groups, the animals were treated with Vertigoheel® 3 times per week for 8 weeks. The drug was injected intraperitoneally, and the dosage was 2ml/kg. In the control groups the animals received no special treatment or placebo.

3.2.3 Cerebral Microvascular Reactivity Assessment

After 8 weeks of therapy with Vertigoheel®, we repeated the cutaneous blood flow measurement using the same procedure. Then the animals were deeply anesthetized by intraperitoneal injection of an anesthetic mixture containing: Fentanyl (0.03 mg/100gr) (Janssen Cilag GmbH, Neuss, Germany), Medetomidine hydrochloride (Domitor vet, 0.01 mg/100gr) (Orion corp., Espoo, Finland), and Midazolam (0.5mg/100gr) (Ratiopharm GmbH, Ulm, Germany). The animals were tracheotomized and artificially ventilated (Animal Respirator Advanced 4601-1, TSE systems GmbH, Bad Homburg, Germany) with room air. The ventilator settings were adjusted until normal arterial blood gas values (pO_2 90 to 105 mmHg; pCO_2 30 to 38 mmHg; pH 7.4) were obtained from the blood sample. Catheters were inserted into the left carotid artery and the left external jugular vein for the measurement of arterial blood pressure, blood gases, and pH and for the infusion of drugs, respectively. Body temperature was maintained at 37 ± 0.5°C with a heating pad. The animals were placed in the prone position. A closed cranial window technique was used, as previously described in detail (74). Briefly, the parietal skull was exposed via a midline incision, after removing the scalp, connective tissue, and muscle. A 3 mm diameter hole was drilled with a multitool drill (Dremel 300 series, Breda, Netherland) in the right anterior parietal bone, 4 mm lateral and 2 mm caudal to the bregma. During the drilling process the skull was continuously cooled with saline to prevent heat damage. Skull bleeding was controlled by the use of bone wax (Serag Wiessner, Germany). The skull was thinned to translucency. Bone that was already thin enough was removed with a forceps and the dura mater was exposed but left intact. The LDF probe (Probe 308, Perimed, Stockholm, Sweden) was positioned above the hole and lowered with a micromanipulator without touching the dura mater. It was positioned thus that visible larger pial vessels were avoided. Saline at 37.5^{o}C was instilled between the probe and the hole, to prevent drying of the dura mater and to improve the optic coupling of the LDF. Cerebral blood flow (CBF) was recorded for 5 minutes as baseline. After the baseline period a blood sample for blood gas analysis was drawn, respiratory hypercapnia was induced by streaming a gas mixture with 5% CO_2 gas through the ventilator. CBF was recorded for 30 minutes, using Scope software (Scope version 2.2.0.30©

2000 Data Translation Inc, Bietiheim-Bissingen, Germany). When the CBF reached its peak, another blood sample was drawn for blood gas analysis. After the measurement of CBF, the animals were euthanized under anesthesia, and the brain was collected and immediately put in liquid nitrogen and stored at -80ºC until measurements. Data was analyzed with Chart5 for windows software (ADInstruments, Oxford, United Kingdom). The CBF increase from normocapnia to hypercapnia was determined. The cerebral microvascular reactivity (CMVR) was calculated as the percent increase of normocapnic to hypercapnic CBF normalized by the change in pCO_2. The cerebrovascular resistance (CVR) was calculated by mean arterial pressure divided by CBF.

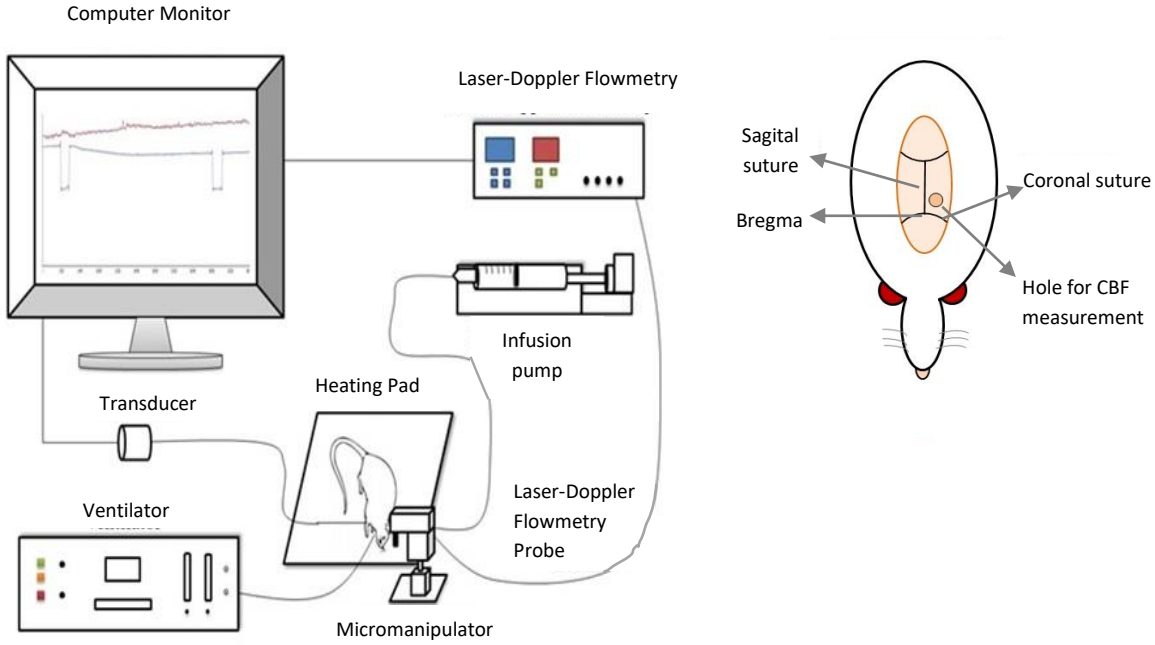

Fig. 7: Schematic diagram of the cerebral blood flow measurement

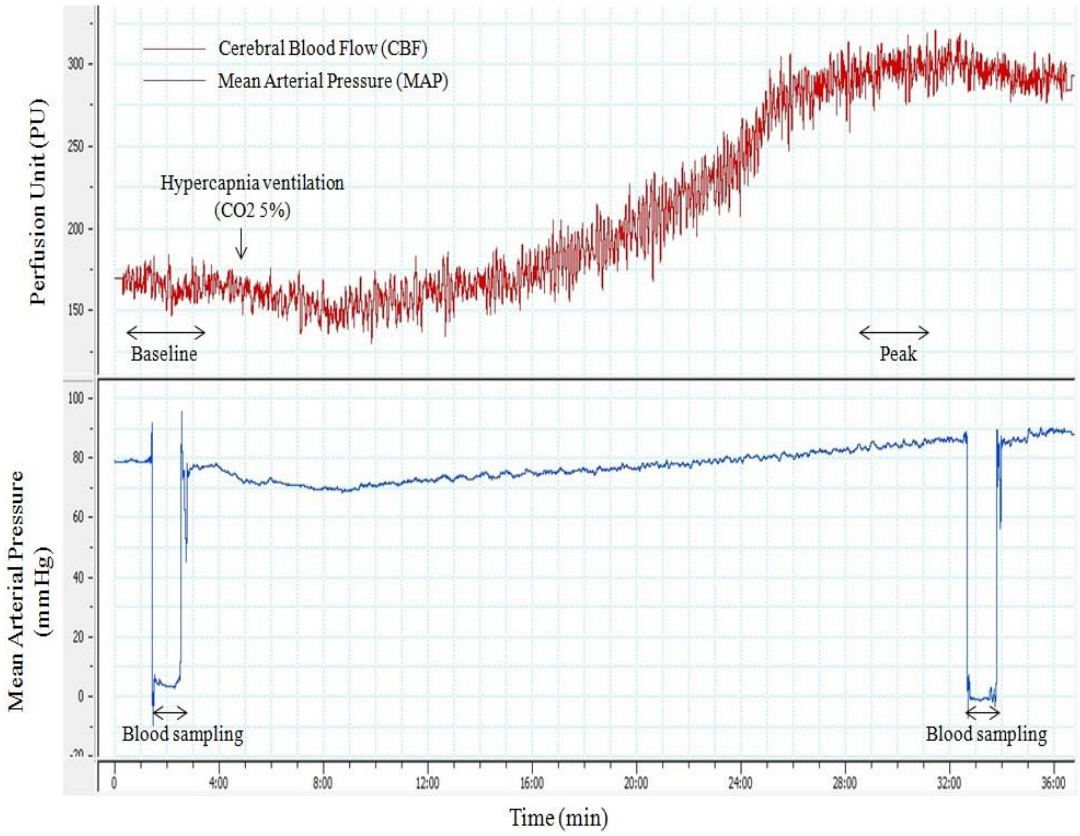

Fig. 8: Example of CBF assessment measured by LDF during hypercapnia

3.2.4 Western Blot

The Western blot method was used, as previously described in detail (75). Briefly, brain tissues were homogenised in a 1:1 (weight:volume) ratio of Extraction Buffer (1 tablet protease inhibitor cocktail complete (Roche, Basel, Switzerland), PBS 9.4 ml, 100 µl PMSF (Sigma-Aldrich, Taufkirchen, Germany), 500 µl Triton X (Sigma-Aldrich, Taufkirchen, Germany)). The homogenate underwent a freeze-thaw cycle three times then centrifugation at 14,000 rpm for 10 min at 4ºC, and the supernatant was recovered. The supernatants were frozen in liquid nitrogen and stored at -80ºC until used. Protein concentrations were measured with BCA protein assay (Pierce® BCA protein assay kit, Thermo Fisher Scientific GmbH, Darmstadt, Germany). Aliquots of the samples, containing equal amounts of proteins (100 µg for eNOS and PDE4D, 10 µg for PDE5A), were suspended in reducing SDS-PAGE sample buffer and heated to 95 °C for 3 minutes. Proteins were loaded to 8% SDS-PAGE gels and separations were carried out with an electrophoresis system (Bio-rad Laboratories GmbH, Munich, Germany). The gels were transferred with a semi-dry transfer system (Bio-rad Laboratories GmbH, Munich, Germany) to a nitrocellulose membrane (Protran BA83, GE Healthcare Life Sciences, Freiburg, Germany)

and then blocked with 5% nonfat dry milk in PBST (Phosphate buffer saline and 0.1% Tween 20) for 2 h. The membrane was then incubated overnight at 4°C with rabbit IgG polyclonal primary antibody at dilutions of 1:500 for eNOS (sc-8311, Santa Cruz Biotechnology, Dallas, Texas, United States), 1:2000 for PDE5A (sc 32884, Santa Cruz Biotechnology, Dallas, Texas, United States), and 1:1000 for PDE4 (ab 14628, Abcam Biotechnology, Cambridge, United Kingdom) subsequently washed with PBST 3 x 5 minutes. The membrane was then incubated with goat anti-rabbit IgG horseradish peroxidase-conjugated secondary antibody (1:10000 for eNOS, 1:20000 for PDE5A; sc 2004, and 1:20000 for PDE4; ab 97051) for 45 minutes. The membrane was developed using a chemiluminescent system (Amersham ECL plus™ Western Blotting Detection Reagent, GE Health Care Life Sciences, Freiburg, Germany) after being washed 5 x 5 minutes with PBST. The optical density for each band was scanned and quantified using ImageJ 1.48v (Wayne Rasband, National Institutes of Health, Bethesda, United States).

3.2.5 ELISA

Brain tissues were homogenized in a 1:1 (weight:volume) ratio of Extraction Buffer (1 tablet protease inhibitor cocktail complete (Roche, Basel, Switzerland), PBS 9,4 ml, 100 µl PMSF (Sigma-Aldrich, Taufkirchen, Germany), 500 µl Triton X (Sigma-Aldrich, Taufkirchen, Germany)). The homogenate underwent a freeze-thaw cycle three times followed by centrifugation at 14,000 rpm for 10 min at 4°C, and the supernatant was recovered. The supernatants were frozen in liquid nitrogen and stored at -80°C until used. Intracellular cAMP & cGMP levels were measured using a commercial ELISA kit (Parameter cAMP assay KGE002B, Parameter cGMP assay KGE003, R&D Systems, Minneapolis, Minnesota, United States) according to the manufacturer's instructions. The samples were diluted 10 times for cAMP and used undiluted for cGMP. The results were calculated with Sigma Plot (Sigma Plot 11.0, Systat Software GmbH, Erkrath, Germany).

3.2.6 Statistical Analyses

For assessment of skin microvascular reactivity, the fold increase between baseline and peak perfusion induced by drug application was evaluated. For the CBF increase assessment, the percent increase of CBF between baseline and peak induced by hypercapnia was used. Optical density data from Western blots were normalized to the GAPDH optical density as a loading control. Data were analyzed with Mann-Whitney U-test for comparison between two groups and

ANOVA on ranks followed by Dunn's or Tukey's tests for comparison among four groups (Sigma Plot 11.0, Systat Software GmbH, Erkrath, Germany). Correlations were analyzed by Spearman rank order test (Sigma Plot 11.0, Systat Software GmbH, Erkrath, Germany). Data are expressed as means ± SE. P-values less than 0.05 were considered to indicate statistically significant differences.

4 Results

4.1 Skin Microvascular Reactivity Assessment

The data obtained at the beginning of the study are summarized in table 3. The baseline body weights in all groups were ± 300 gr. To confirm the endothelial and vessel wall dysfunction in SHR, we assessed the reactivity of the skin microvascular response to ACh and SNP. All groups showed responses to ACh and SNP in the skin microvascular reactivity assessment. Yet, the response to both ACh and SNP in the SHR groups was significantly smaller than in the WKY groups (Fig. 9, 10).

Table 3**:** Baseline general data

	SHR-V (n=16)	SHR-C (n=15)	WKY-V (n=16)	WKY-C (n=15)
Body weight	312.13 ± 2.41*	324.53 ± 2.97§	358 ± 5.24	365.93 ± 3
Skin perfusion fold increase (ACh)	3.7 ± 0.7*	3.8 ± 0.3§	5.5 ± 0.6	5.6 ± 0.7
Skin perfusion fold increase (SNP)	5.0 ± 0.7*	4.1 ± 0.4§	8.0 ± 0.7	10.5 ± 3.3

SHR-V, Spontaneously Hypertensive Rat Vertigoheel® treated group; SHR-C, Spontaneously Hypertensive Rat control group; WKY-V, Wistar- Kyoto Vertigoheel® treated group; WKY-C, Wistar-Kyoto control group; Ach, Acetylcholine; SNP, Sodium nitroprusside. Data are mean ± SE. *p<0.05 vs WKY-V, §p<0.05 vs WKY-C

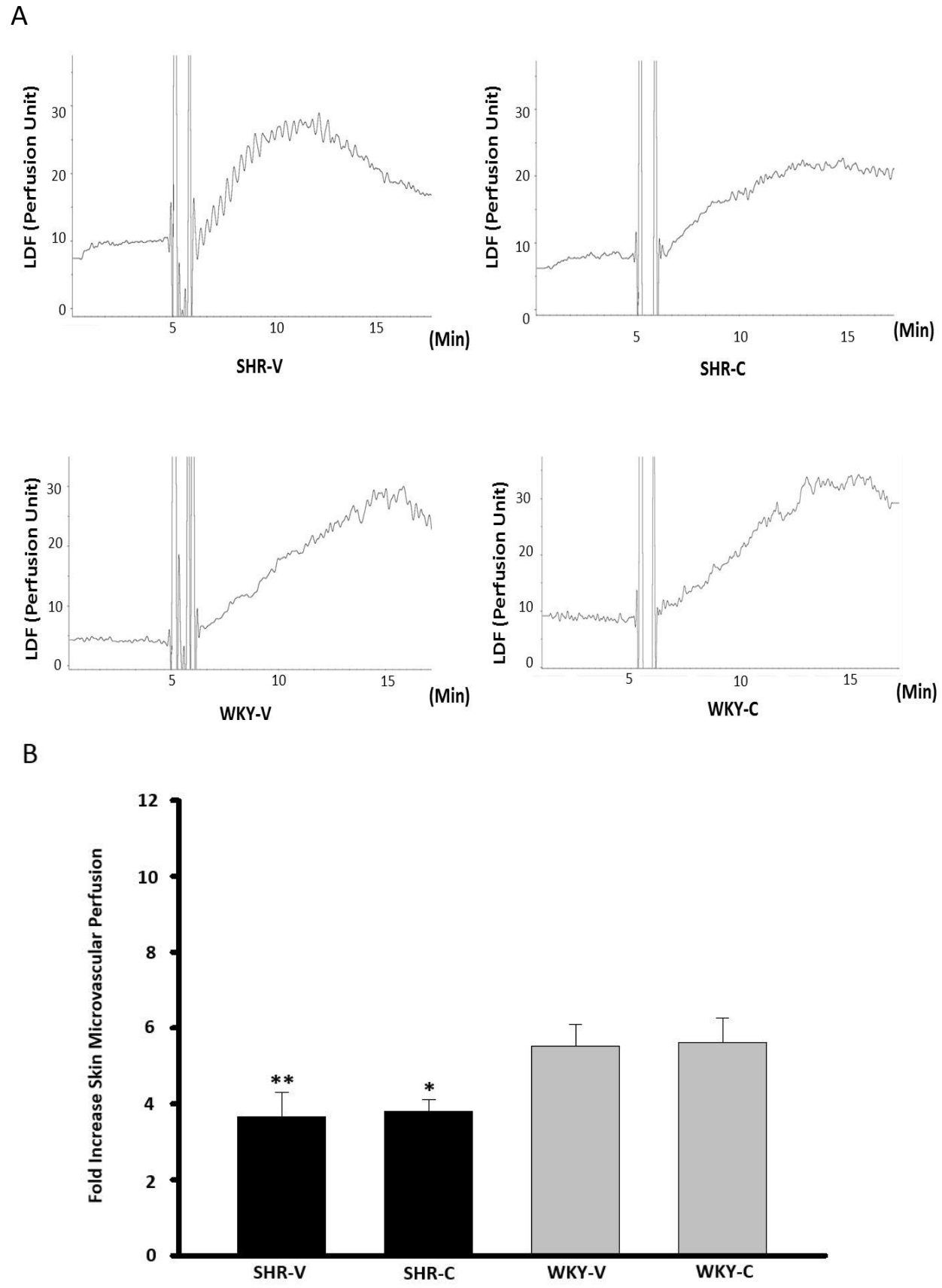

Fig.9: First skin microvascular assessment with Acetylcholine (ACh) stimulation before Vertigoheel® treatment. A. Representative examples of laser-Doppler flowmetry (LDF) 2% ACh stimulation. B. Quantification of LDF shows that skin perfusion increase is significantly reduced in Spontaneously Hypertensive Rats Control (SHR-C) and Vertigoheel® (SHR-V) groups compared to Wistar Kyoto Rat Control (WKY-C) and Vertigoheel® (WKY-V) groups. (n=15 SHR-V, n=15 SHR-C, n=16 WKY-V, n=15 WKY-C. *p<0.05 vs WKY-C, **p<0.005 vs WKY-V).

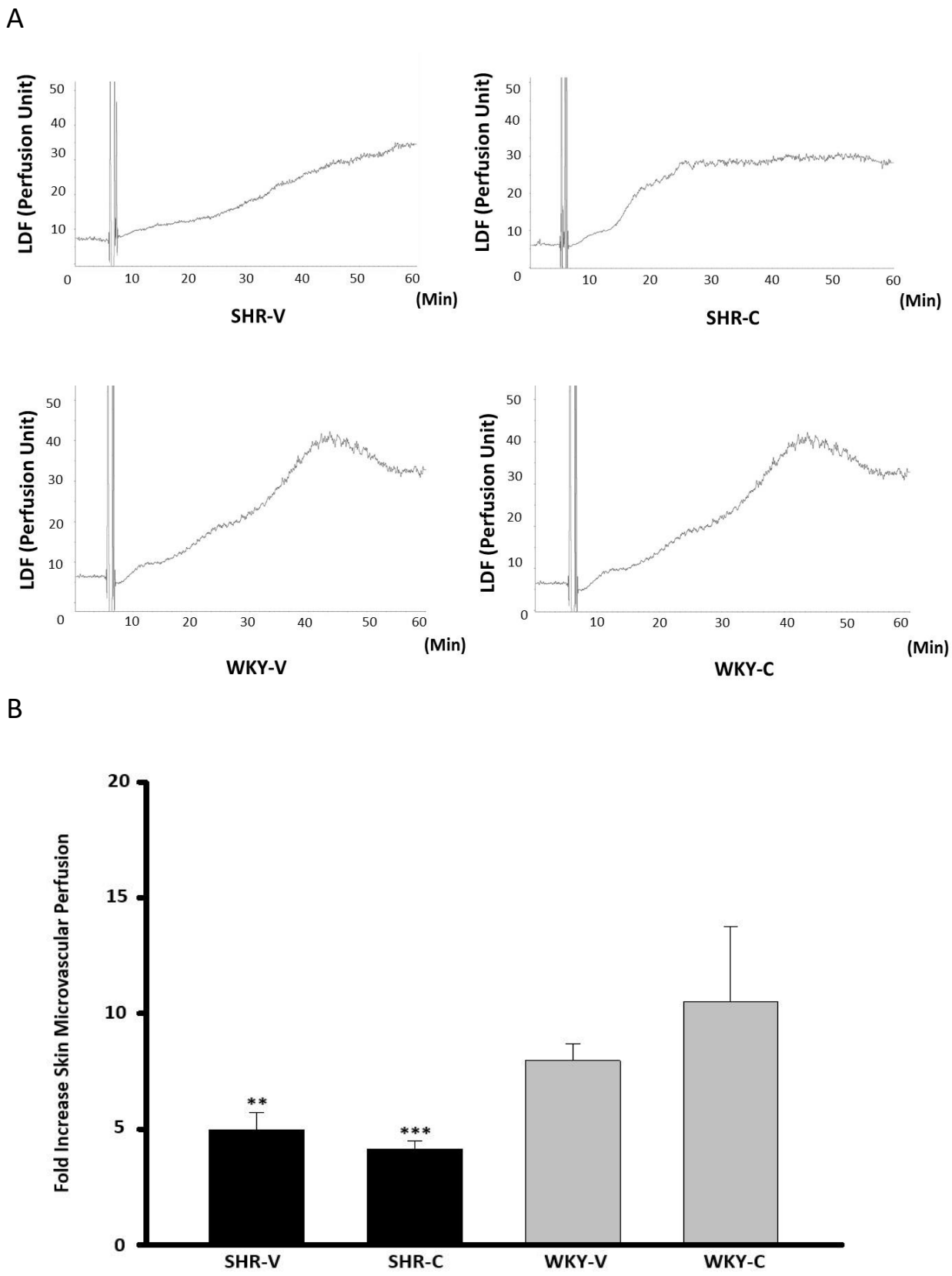

Fig. 10: First skin microvascular assessment with Sodium Nitroprusside (SNP) stimulation before Vertigoheel® treatment. A. Representative examples of laser-Doppler flowmetry (LDF) with 2% SNP stimulation. B. Quantification of LDF shows that skin perfusion is significantly reduced in Spontaneously Hypertensive Rats Control (SHR-C) and Vertigoheel® (SHR-V) groups compared to Wistar Kyoto Rat Control (WKY-C) and Vertigoheel® (WKY-V) groups. (n=15 WKY-C, n=16 WKY-V, n=15 SHR-C, n=15 SHR-V. **p<0.005 vs WKY-V, ***p<0.001 vs WKY-C).

After 8 weeks of treatment with Vertigoheel® we reassessed the baseline data as summarized in table 4. The body weight of the WKY groups at the end of the experiment was significantly higher compared to SHR groups. In the skin microvascular reactivity assessment, we observed that there was no significant difference found between SHR and WKY or either between SHR-V and SHR-C or WKY-V and WKY-C in response to ACh (Fig. 11). However, we observed a higher response of SNP induced skin microvascular vasodilation in WKY-V compared to WKY-C which was not seen between SHR-V and SHR-C (Fig. 12).

Table 4: General data after 8 weeks treatment procedure

	SHR-V (n=16)	SHR-C (n=15)	WKY-V (n=16)	WKY-C (n=15)
Body weight	368.5 ± 3.84*	378.4 ± 4.26§	441.81±6.84	435.8 ± 4.31
Skin perfusion fold increase (Ach)	4.1 ± 0.4	4.8 ± 0.6	4.4 ± 0.5	5.3 ± 0.7
Skin perfusion fold increase (SNP)	5.5 ± 0.4*	7.0 ± 0.7	8.5 ± 0.7	6.6 ± 0.6

SHR-V, Spontaneously Hypertensive Rat Vertigoheel® treated group; SHR-C, Spontaneously Hypertensive Rat control group; WKY-V, Wistar- Kyoto Vertigoheel® treated group; WKY-C, Wistar-Kyoto control group; Ach, Acetylcholine; SNP, Sodium nitroprusside. Data are mean ± SE. *p <0.05 vs WKY-V, §p <0.05 vs WKY-C.

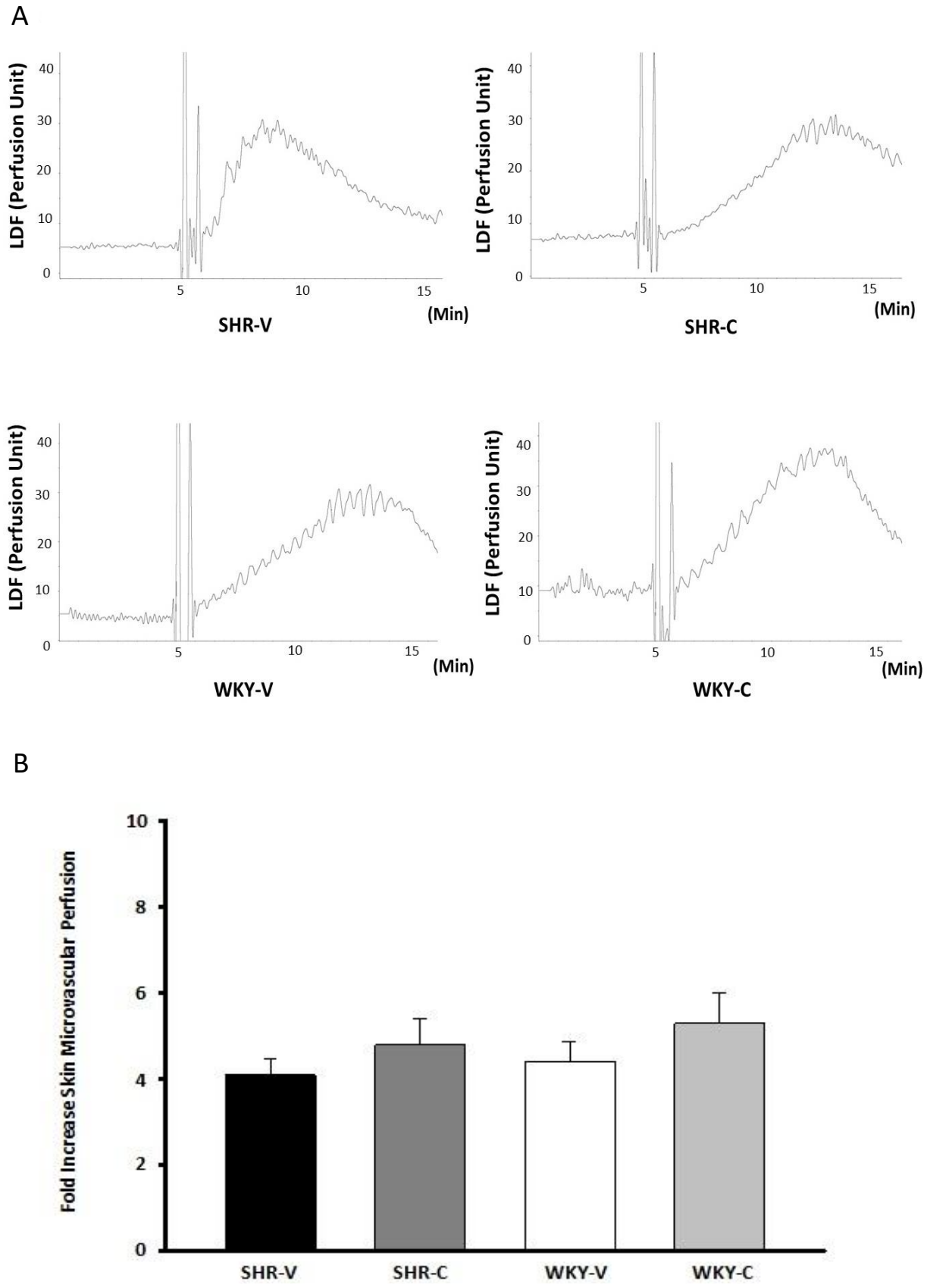

Fig. 11: Second skin microvascular assessment with Acetylcholine (ACh) stimulation after 8 weeks Vertigoheel® treatment. A. Representative examples of laser-Doppler flowmetry (LDF) with 2% ACh stimulation. B. Quantification of LDF shows no significant differences in skin perfusion responses of Wistar Kyoto Rats Control (WKY-C), Wistar Kyoto Rats Vertigoheel® treated (WKY-V), Spontaneously Hypertensive Rats Control (SHR-C), or Spontaneously Hypertensive Rats Vertigoheel® treated (SHR-V) groups. (n=15 SHR-V, n=15 SHR-C, n=16 WKY-V, n=15 WKY-C).

A

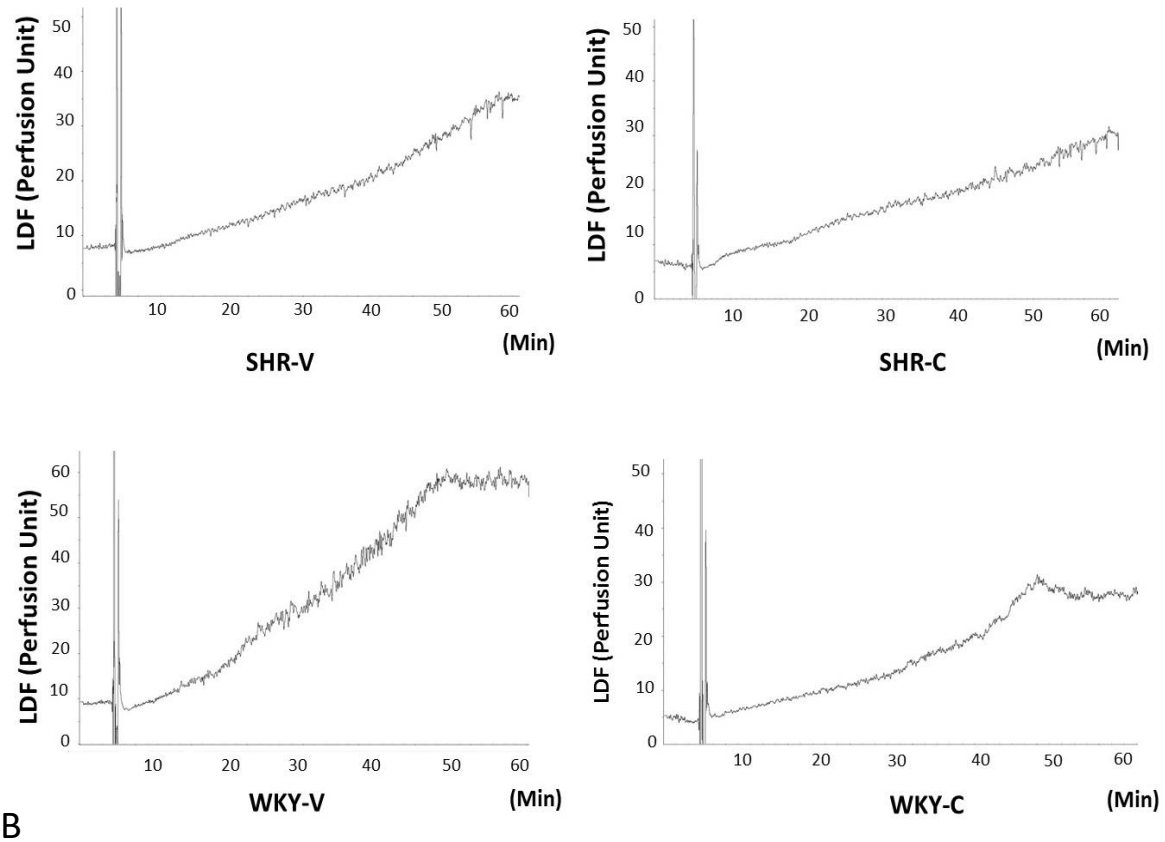

B

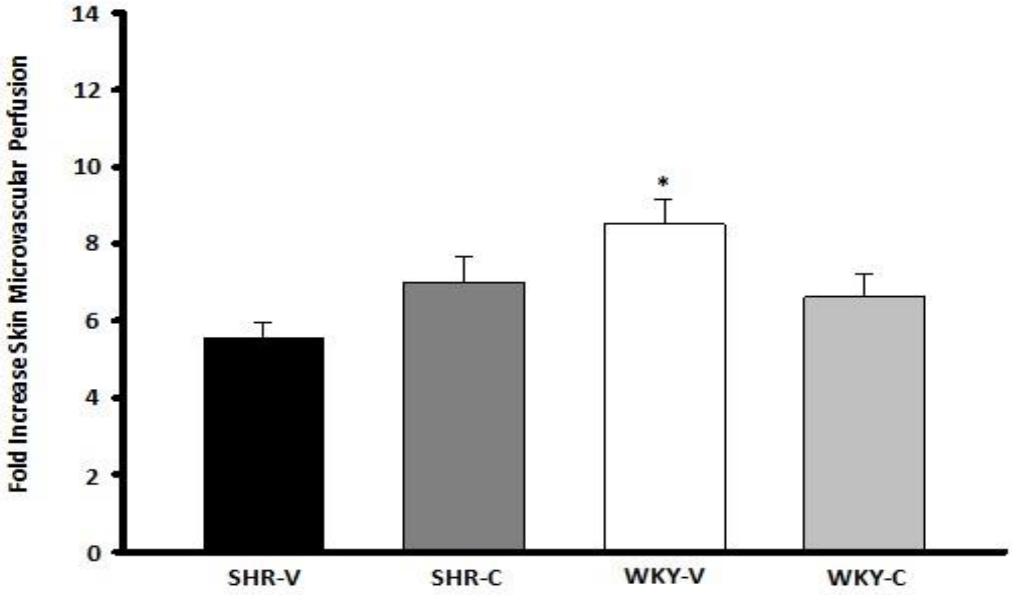

Fig. 12: Second skin microvascular assessment with Sodium Nitroprusside (SNP) stimulation after 8 weeks Vertigoheel® treatment. A. Representative examples of laser-Doppler flowmetry (LDF) with 2% SNP stimulation. B. Quantification of LDF shows no significant difference in skin perfusion between Spontaneously Hypertensive Rats Control (SHR-C) and Spontaneously Hypertensive Rats Vertigoheel® treated (SHR-V) group. Wistar Kyoto Rats Vertigoheel® treated (WKY-V) group shows moderately increased perfusion response compared to Wistar Kyoto Rats Control (WKY-C) group and Spontaneously Hypertensive Rats Vertigoheel® treated (SHR-V) group. (n=15 SHR-V, n=15 SHR-C, n=16 WKY-V, n=15 WKY-C). *p<0.05 vs SHR-V

4.2 Cerebral Microvascular Reactivity Assessment

To assess the effect of Vertigoheel® on the cerebral microvascular function, we measured the CMVR to hypercapnia with LDF. Hypercapnia-induced cerebral microvascular vasodilation increased cerebral microvascular perfusion in all groups (Fig. 13). Increase in cerebral microvascular perfusion typically occurred after 15 minutes of mild hypercapnic ventilation. In the WKY groups and the SHR-V group the peak perfusion increase was about 50% compared to baseline. Interestingly, the increase of cerebral microvascular perfusion in the SHR-C group was only 20% compared to baseline. The increase in cerebral microvascular perfusion in SHR-V was significantly greater compared to SHR-C. There was no significance difference between WKY-V and WKY-C (Fig. 14).

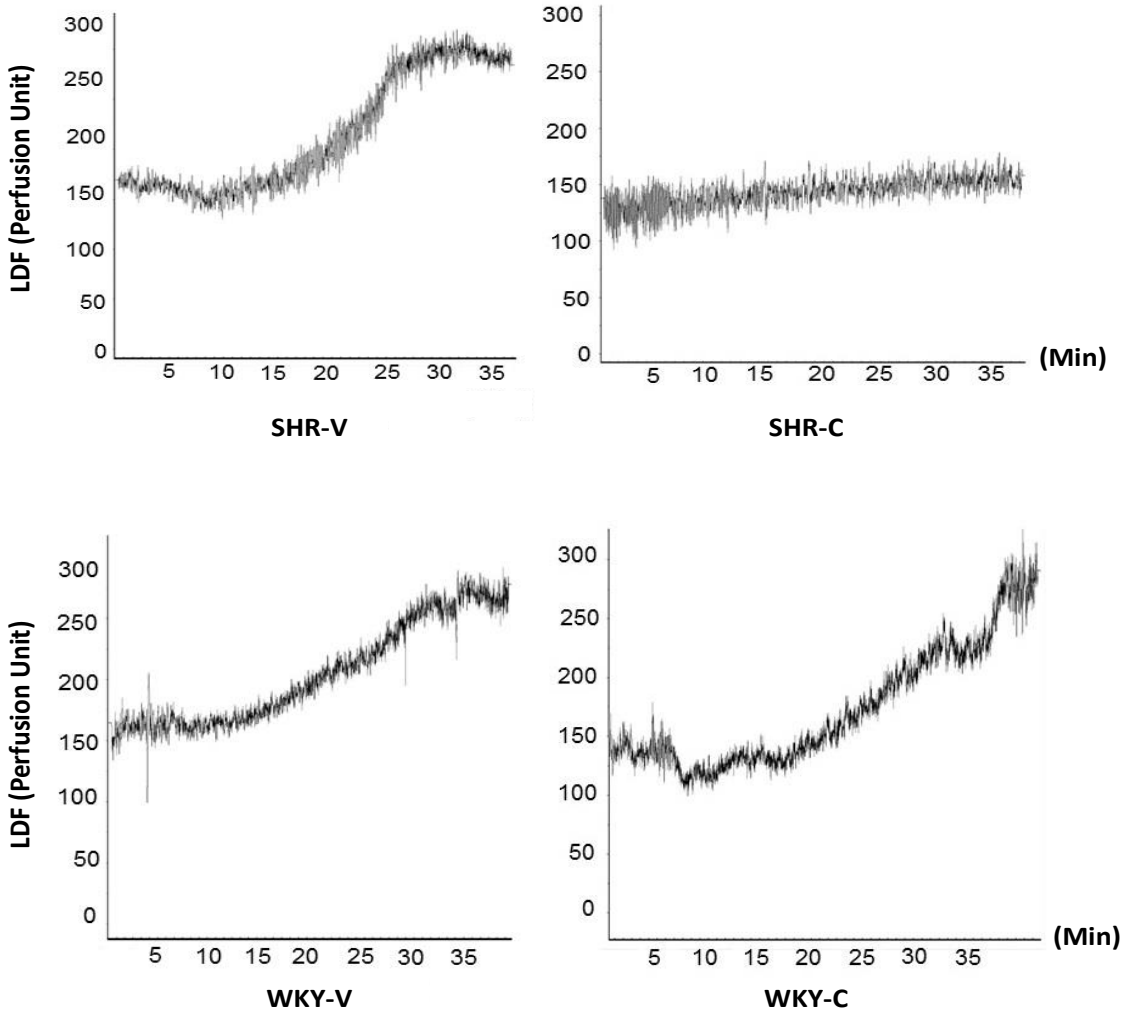

Fig. 13: Representative picture from cerebral microvascular reactivity assessment with mild hypercapnia stimulation measured by laser-Doppler flowmetry (LDF) in perfusion unit (PU) after 8 weeks Vertigoheel® treatment.

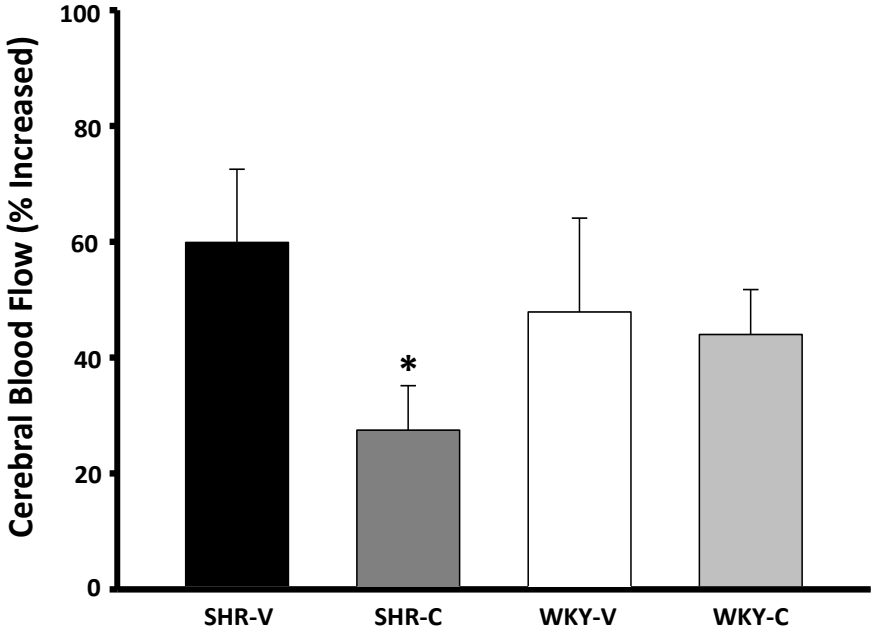

Fig. 14: Quantification of LDF shows that cerebral perfusion response to hypercapnia is significantly reduced in Spontaneously Hypertensive Rats Control (SHR-C) compared to the Spontaneously Hypertensive Rats Vertigoheel® treated (SHR-V) group. (n=13 SHR-V, n=11 SHR-C, n=9 WKY-V, n=14 WKY-C. *p<0.05 vs SHR-V).

Table 5 shows the parameters that were assessed in cerebral microvascular reactivity assessment and the absolute numbers of CBF in perfusion units. Under normocapnia condition the pH was 7.39±0.02 – 7.40±0.02. This pH condition was decreased to 7.22±0.01 – 7.23±0.02 following the mild hypercapnia ventilation. Under normocapnia condition, the pCO_2 was 34.6±1.5 – 38.3±0.7 and it was increased to 57.2±2.3 – 65.5±2.1 when the ventilation changed into mild hypercapnia. The pO_2 in normocapnia and mild hypercapnia condition was relatively stable. The pO_2 was 90±4 - 107±7 and 92±5 - 117±9 under normocapnia and mild hypercapnia condition, respectively. The MAP and cerebrovascular resistance index (RI) in SHR-C were significantly higher compared to WKY-C in normocapnia and hypercapnia condition suggesting higher baseline blood pressure and increases peripheral resistance in SHR. Interestingly, the percent increase of CBF was significantly lower in SHR-C compared to SHR-V. Furthermore, the CMVR response to hypercapnia in SHR-C was significantly lower compared to SHR-V and WKY-C.

Table 5: Cerebral microvascular reactivity parameter

		SHR-V (n=13)	SHR-C (n=11)	WKY-V (n=9)	WKY-C (n=14)
pH	Normocapnia	7.40 ± 0.02	7.40 ± 0.01	7.38 ± 0.01	7.39 ± 0.02
	Hypercapnia	7.23 ± 0.02	7.22 ± 0.01	7.23 ± 0.02	7.22 ± 0.01
pCO_2 [mmHg]	Normocapnia	38 ± 1	38 ± 1	35 ± 1	35 ± 2
	Hypercapnia	61 ± 2	66 ± 2	57 ± 2	57 ± 2
pO_2 [mmHg]	Normocapnia	93 ± 4	107 ± 7	100 ± 6	90 ± 4
	Hypercapnia	101 ± 5	117 ± 9	104 ± 8	92 ± 5
MAP [mmHg]	Normocapnia	92 ± 7	107 ± 7§	70 ± 7	51 ± 2
	Hypercapnia	91 ± 8	89 ± 3§	72 ± 7	60 ± 4
RI	Normocapnia	0.6± 0.06	0.7± 0.08§	0.5± 0.08	0.3± 0.02
	Hypercapnia	0.4± 0.03	0.4± 0.05§	0.3± 0.03	0.3± 0.02
CBF [PU]	Normocapnia	158 ± 12	176 ± 17	165 ± 14	160 ± 11
	Hypercapnia	241 ± 15	221 ± 21	237 ± 20	226 ± 15
Difference					
Delta % CBF		60 ± 13	27 ± 8*	48 ± 16	44 ± 8
Delta pCO_2		23 ± 2	27 ± 2	22 ± 2	23 ± 1
CMVR (%/mmHg)		2.8 ± 0.6	1.0 ± 0.3*§	2.0 ± 1	2.2 ± 0.4

SHR-V= Spontaneously Hypertensive Rats Vertigoheel® treated group; SHR-C= Spontaneously Hypertensive Rats control group; WKY-V= Wistar-Kyoto Vertigoheel® treated group; WKY-C= Wistar-Kyoto control group; pH= Activity of Hydrogen ion; pO_2= arterial oxygen tension; pCO_2= arterial carbon dioxyde tension; MAP= mean arterial pressure; CBF= cerebral blood flow in perfusion units; RI= cerebrovascular resistance index, CMVR= cerebral microvascular reactivity.*$p<0.05$ vs SHR-V, §$p<0.05$ vs WKY-C.

4.3 Western Blot

To investigate the putative mechanism by which Vertigoheel® may increase CMVR, the expression of eNOS, PDE5, and PDE4 in tissue homogenate was determined. The Western blot results in this study showed downregulation of eNOS protein expression in cerebral tissue in SHR-C compared to WKY-C. After 8 weeks of Vertigoheel® treatment, eNOS protein expression showed significant upregulation in SHR-V compared to SHR-C. The level of eNOS protein expression in SHR-V was almost the same as in WKY-V and WKY-C. There was no significant difference between WKY-C and WKY-V (Fig. 15).

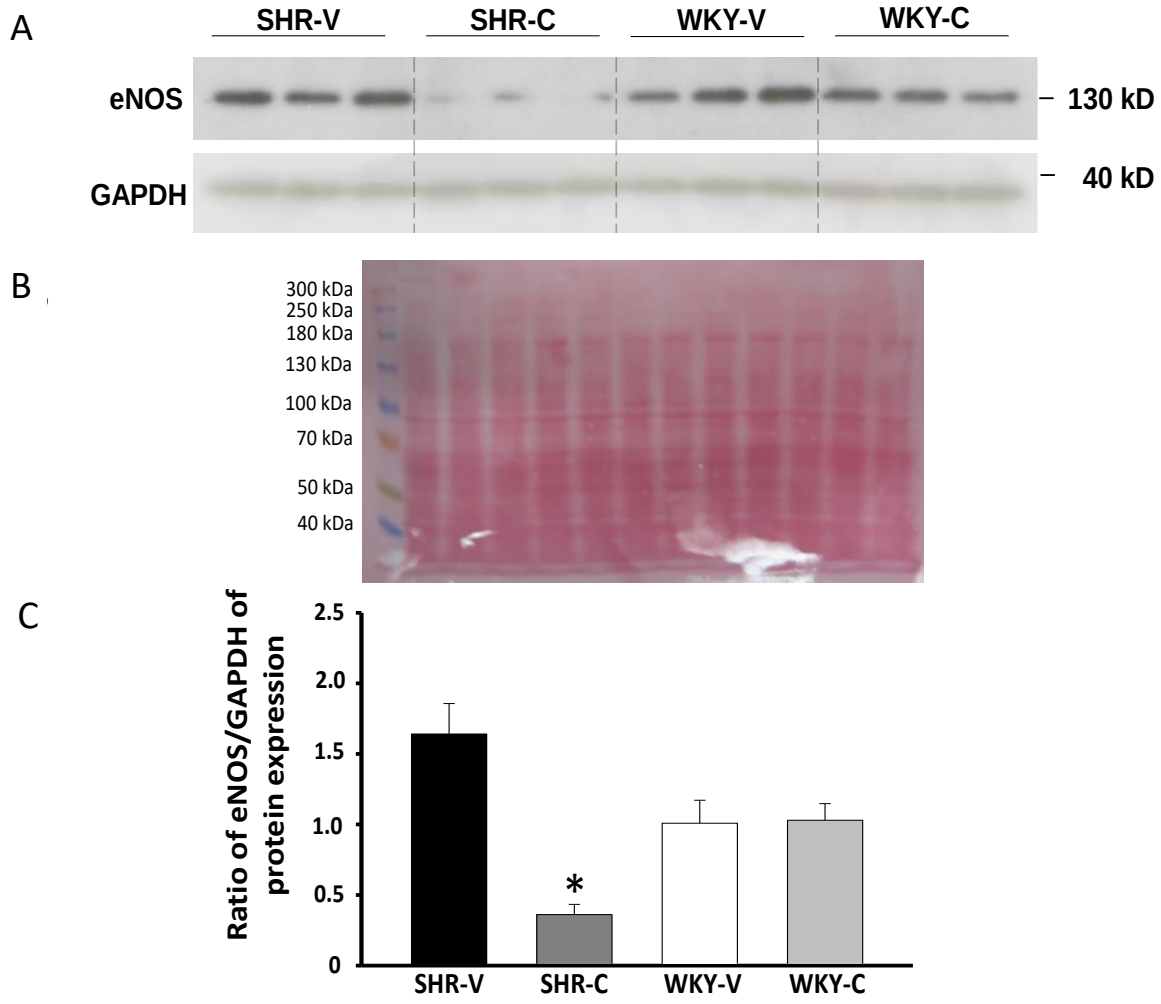

Fig. 15: Effect of Vertigoheel® on eNOS expression. A. Representative blot from eNOS in cerebral homogenate from Spontaneously Hypertensive Rats Vertigoheel® treated (SHR-V) (n=3), Spontaneously Hypertensive Rats control (SHR-C) (n=3), Wistar Kyoto Rats Vertigoheel® treated (WKY-V) (n=3) and Wistar Kyoto Rats control group (WKY-C) (n=3). The molecular mass of eNOS is approximately 130 kDa. GAPDH as protein loading control showed equal protein loading. The molecular mass of GAPDH is approximately 37 kDa. B. Ponceau protein stain of the transfer membrane showed equal protein loading. C. Quantification of Western blot by normalizing eNOS with GAPDH optical density showed that eNOS expression in SHR-C was significantly lower compared to SHR-V and WKY-C. No significant difference in SHR-V compared to WKY-V and WKY-C. Data in mean ± SEM. (n=6 SHR-V, n=6 SHR-C, n=6 WKY-V, n=6 WKY-C. *$p<0.05$ vs SHR-V and WKY-C).

Western blot expression for PDE5 showed no significance difference between SHR-V and SHR-C. There was also no significance difference between WKY-V and WKY-C (Fig. 16).

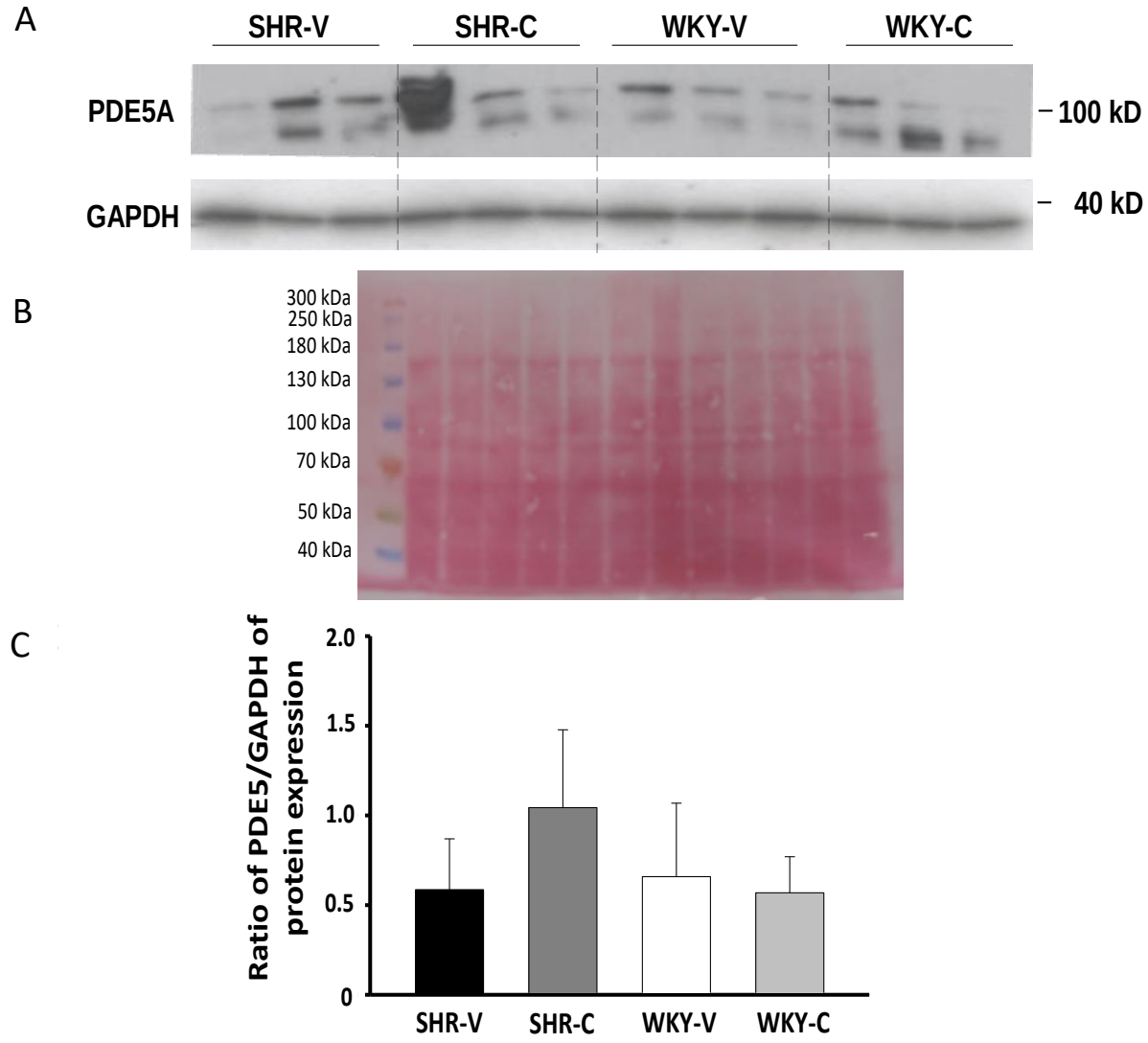

Fig. 16: Effect of Vertigoheel® on PDE5 expression. A. Representative blot from PDE5A in cerebral homogenate from Spontaneously Hypertensive Rats Vertigoheel® treated (SHR-V) (n=3), Spontaneously Hypertensive Rats control (SHR-C) (n=3), Wistar Kyoto Rats Vertigoheel® treated (WKY-V) (n=3) and Wistar Kyoto Rats control group (WKY-C) (n=3). The molecular mass of PDE5A is approximately 100 kDa. GAPDH as protein loading control showed equal protein loading. The molecular mass of GAPDH is approximately 37 kDa. B. Ponceau protein stain of the transfer membrane showed equal protein loading. C. Quantification of Western blot by normalizing PDE5A with GAPDH optical density showed no significant difference in PDE5A expression among groups. Data in mean ± SEM. (n=6 SHR-V, n=6 SHR-C, n=6 WKY-V, n=6 WKY-C).

Besides eNOS and PDE5, we also examined cerebral PDE4 expression with Western blotting. Cerebral PDE4 expression showed no significant difference between SHR-C and SHR-V. There was no significant difference between WKY-V and WKY-C (Fig. 17).

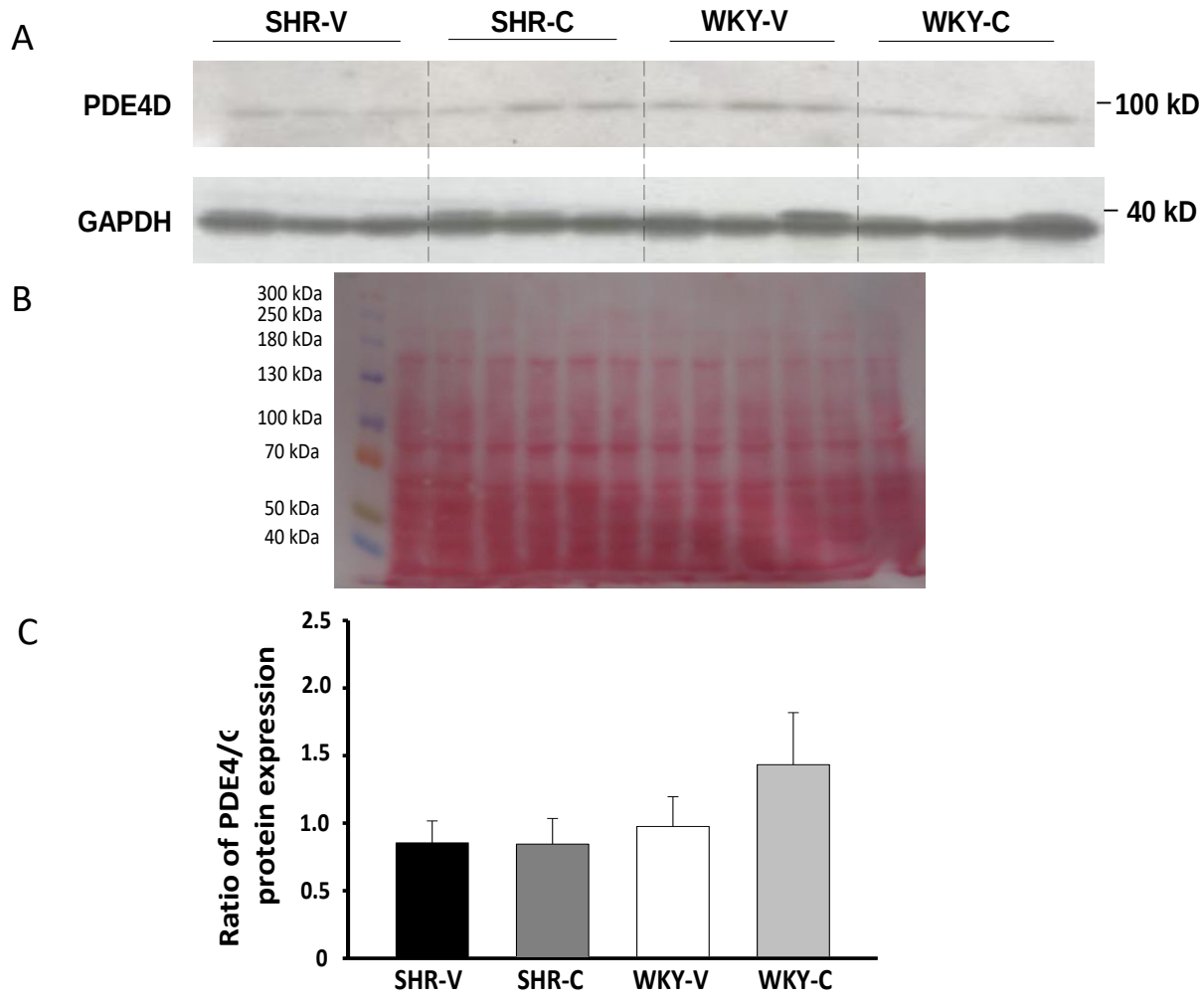

Fig. 17: Effect of Vertigoheel® on PDE4 expression. A. Representative blot from PDE4D in cerebral homogenate from Spontaneously Hypertensive Rats Vertigoheel® treated (SHR-V) (n=3), Spontaneously Hypertensive Rats control (SHR-C) (n=3), Wistar Kyoto Rats Vertigoheel® treated (WKY-V) (n=3) and Wistar Kyoto Rats control group (WKY-C) (n=3). The molecular mass of PDE4D is approximately 70 kDa. GAPDH as protein loading control showed equal protein loading. The molecular mass of GAPDH is approximately 37 kDa. B. Ponceau protein stain of the transfer membrane showed equal protein loading. C. Quantification of Western blot by normalizing PDE4D with GAPDH optical density showed no significant difference in PDE4D expression among groups. Data in mean ± SEM. (n=6 SHR-V, n=6 SHR-C, n=6 WKY-V, n=6 WKY-C).

4.4 ELISA

cAMP and cGMP play a major role as smooth muscle cell second messengers in vasodilatory mechanisms. We, therefore, assessed the cAMP and cGMP concentrations in cerebral tissue homogenates with ELISA. Table 6 shows absolute cerebral cAMP and cGMP concentrations. Regarding cAMP, there was no significant difference between SHR-V and SHR-C or between WKY-C and WKY-V. cAMP concentration was significantly higher in WKY-C compared to SHR-C.

Regarding cGMP, there was no significant difference between SHR-V and SHR-C. No significant difference was also observed in WKY-C compared with WKY-V. A significantly higher cerebral cGMP concentration was observed in WKY-V compared to SHR-V. There was no significant difference between WKY-C and SHR-C.

Table 6: ELISA cerebral cAMP and cGMP levels

		SHR-V (n=13)	SHR-C (n=11)	WKY-V (n=9)	WKY-C (n=14)
cAMP	pmol/g tissue	370±55	452±77§	528±76	742±198
cGMP	pmol/g tissue	67±10*	88±15	112±16	95±19

SHR-V= Spontaneously hypertensive rats Vertigoheel® treated group; SHR-C= Spontaneously hypertensive rats control group; WKY-V= Wistar Kyoto Vertigoheel® treated group; WKY-C= Wistar kyoto control group. cAMP and cGMP concentrations in pmol/ g tissue. Data is in mean ± SEM. §$p<0.05$ vs WKY-C. * $p<0.05$ vs WKY-V

eNOS plays role in vasodilatory mechanisms. The downstream pathway from eNOS involves cGMP as a second messenger in vascular smooth muscle cells. In addition to cGMP, cAMP also plays role in vascular smooth muscle relaxation. Furthermore, cGMP and cAMP are degraded by PDE5 and PDE4, respectively. We, therefore, tried to correlate the results from eNOS and PDE5 with cGMP and of PDE4 with cAMP. In our study we observed no correlation between cGMP concentrations and eNOS expression (Fig. 18). There was also no correlation found between cGMP concentrations and PDE5 expression (Fig. 19) or between cAMP concentrations and PDE4 expression (Fig. 20).

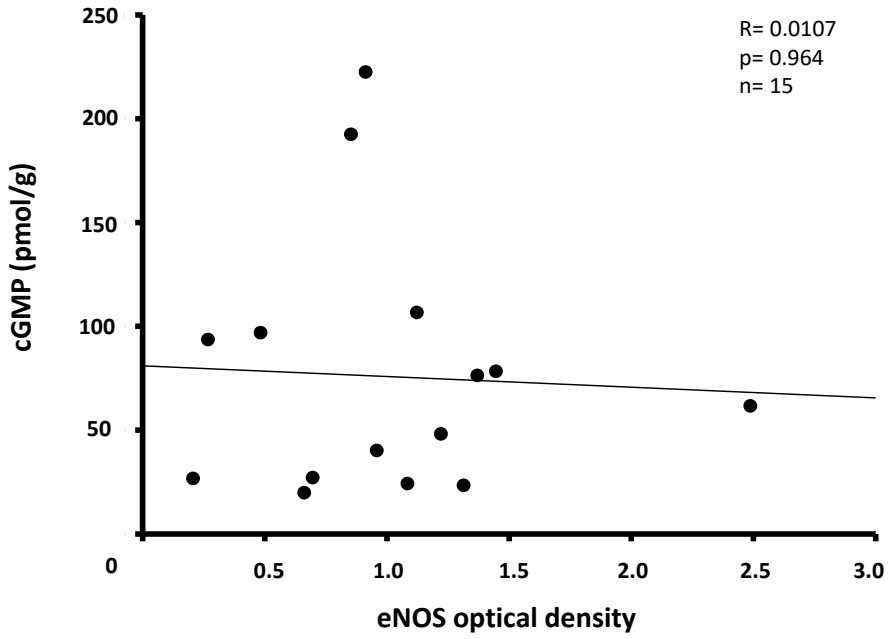

Fig. 18: Correlation of endothelial nitric oxide synthase (eNOS) and cyclic guanosine monophosphate (cGMP). No correlation between endothelial nitric oxide synthase (eNOS) expression and cGMP concentration in cerebral homogenate.

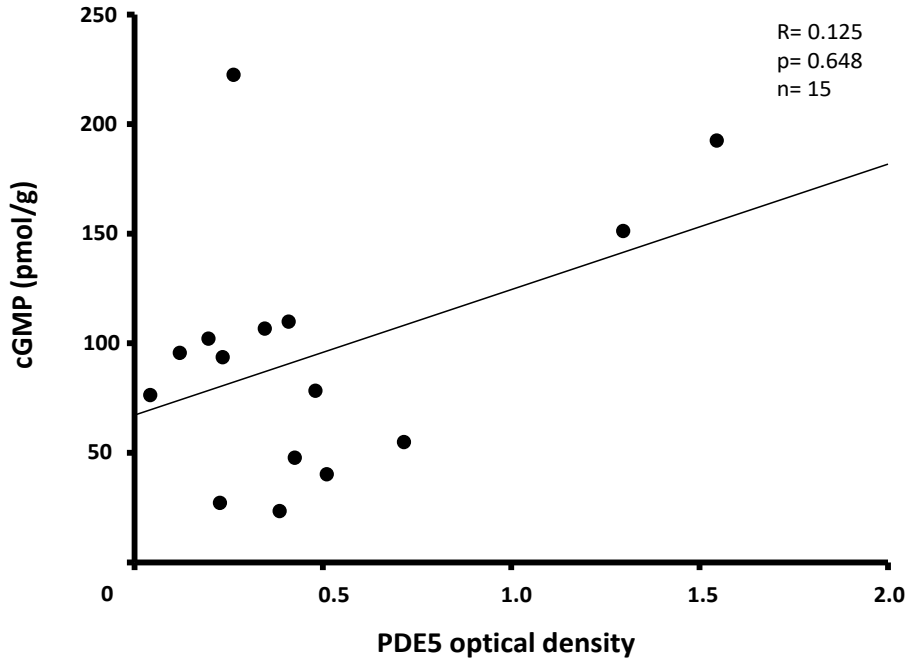

Fig. 19: Correlation of phosphodiesterase 5 (PDE5) and cyclic guanosine monophosphate (cGMP). No correlation between phosphodiesterase 5A (PDE5A) expressions and cGMP concentrations in cerebral homogenates.

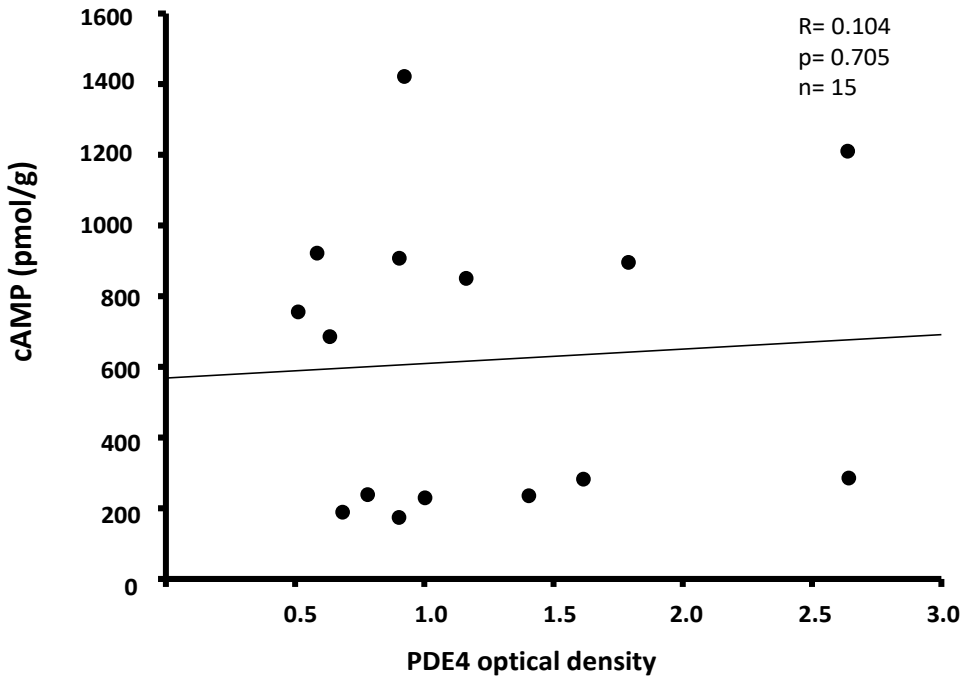

Fig. 20: Correlation of phosphodiesterase 4 (PDE4) and cyclic adenosine monophosphate (cAMP). No correlation between phosphodiesterase 4 (PDE4) expressions and cAMP concentration in cerebral homogenate.

5. Discussion

5.1 Discussion of Methods

In the beginning, a causal relationship between hypertension and endothelial dysfunction has been assumed (76). On the other side, there are also several studies that hypothesized that the endothelial dysfunction precedes the development of hypertension (23). Another theory pointed out that the relationship between hypertension and endothelial dysfunction is not a cause and effect relationship but a cyclical one (76). At the bottom line, basic and clinical studies demonstrated a consistent association between essential hypertension, a major risk for vascular dementia, and endothelial cells disturbance (76-79). Several methods to measure the endothelial dysfunction are quantitative angiography, venous occlusion plethysmography, micromyography, brachial ultra-sound during reactive hyperemia assessing flow-mediated dilation (FMD), peripheral artery tonometry, or LDF (76). In our study we used LDF in rat skin and brain to assess the microvascular responsiveness to ACh, SNP, or hypercapnia, respectively. LDF is a technique to assess microvascular blood flow that can continuously monitor the microcirculation in various tissue types and organs in real-time. When used on skin, LDF evaluates blood flow in capillaries that are close to the surface and the flow in the underlying arterioles and venules involved in the regulation of tissue temperature (80). When LDF is used for assessing the microcirculation of inner organs, surgical preparation is necessary to expose the organ surface.

The measuring principle of LDF relies on the Doppler phenomenon. When a laser beam with at certain wavelength is directed onto the surface of skin or exposed organ tissue, a fraction of the light penetrates through the skin and is reflected by both static and moving cells (i.e red blood cells). Reflection by a moving red blood cells results in a wavelength or frequency shift (the Doppler shift) while light scattered by stationary cells remains unshifted. The backscattered light is transmitted back into the instrument and is transformed into an analog signal by photomultipliers. Analysis of the backscattered light yields the frequency of the Doppler shift, which is proportional to the red cell velocity. The percentage of light energy presenting with such a Doppler shift represents the number of moving red blood cells from which light has been reflected. The output of the LDF is referred to as “perfusion flux” which is proportional to the product of the number of moving blood cells times the mean velocity (81).

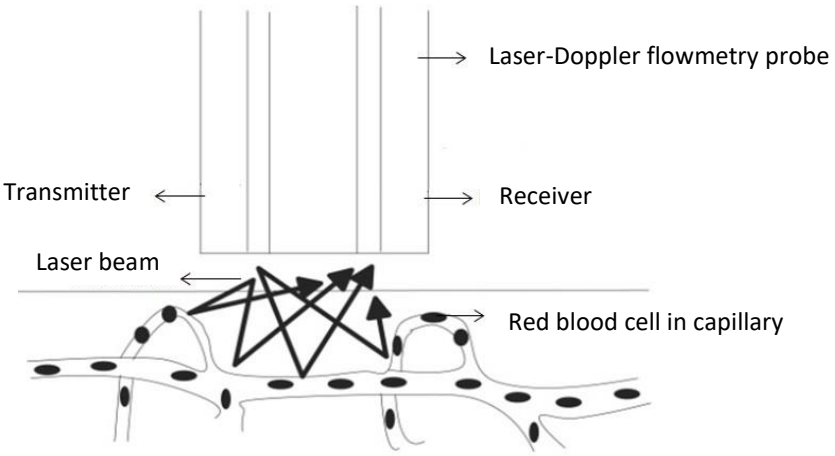

Fig. 21: Schematic diagram of the measurement principle of laser-Doppler flowmetry (82)

In our study, we combined the LDF technique with the SHR as an animal model for cerebral microvascular disturbance. Besides SHR, other animal models for vascular dementia usually involve vessel occlusion, stenosis, or embolization, for example bilateral carotid artery occlusion or embolic intracerebral artery occlusion (83). Compared to these models, the SHR has several advantages. One advantage is that SHR is the rat strain that has been investigated most extensively including assessment of hypertensive cerebral end organ damage and treatment of it. This allows us to compare the results of the present study with previous studies (84). Another advantage of using this animal model for studying vascular cerebral disease is the continuous development of hypertension in SHR. The SHR are born with normal blood pressure and gradually develop hypertension. At the age of 6 months they have a sustained hypertension. The course of this development is similar with essential hypertension in humans, which is the major risk factor for vascular dementia in the later life (18). Moreover, like the hypertension in humans, hypertension in SHR involves global microvascular disturbance throughout the body (67;85). Based on this phenomenon, microvascular measurement in any tissue may be used to assess microvascular disturbance or endothelial dysfunction related with hypertension. In our experiment we used the skin because it was easily accessible for non-invasive measurements of endothelial or generalized microvascular dysfunction related to the hypertension of SHR.

5.2 Discussion of Results

In the present study we demonstrated the effect of Vertigoheel® on cerebral microvascular perfusion of SHR. The main finding of this study is that Vertigoheel® can increase cerebral microvascular perfusion response to a physiological vasodilatory stimulus in SHR. The

increase in cerebral microvascular perfusion response in this group might be related to an increased expression of eNOS compared to the SHR untreated group.

5.2.1 Skin Microvascular Reactivity Assessment

To confirm the endothelial dysfunction related with essential in hypertension in SHR, we measured the baseline endothelial function in SHR and WKY rats. At the baseline LDF assessment, the skin microvascular perfusion in SHR with a smaller vasodilatory response to ACh and SNP compared to WKY, the normotensive control group. This result confirmed the presence of microvascular dysfunction in SHR at the age of 16 weeks, probably due to chronic hypertension. Microvascular dysfunction in this study affected not only the endothelium but also vascular smooth muscle because it was evident not only after stimulation with the endothelium dependent vasodilator ACh but also after stimulation with the endothelium independent vasodilator SNP. In other studies microvascular dysfunction in SHR was only demonstrated after administration of ACh but not SNP (86-89). On the other hand, several studies have demonstrated disturbance of microvascular perfusion in SHR in response to both, ACh and SNP (90-93). These conflicting results could be the caused by differences in the progression or duration of hypertension due to the use of differently aged experimental animals. In the present study, progression and duration of hypertension in SHR already affected vascular smooth muscle function during baseline measurements.

After 8 weeks of treatment with Vertigoheel®, the assessment of skin microvascular perfusion with LDF was repeated, but no improvement in skin microvascular perfusion response was seen in SHR-V compared to SHR-C after stimulation with either ACh or SNP. Interestingly, the difference of ACh stimulated skin microvascular reactivity between the SHR and WKY groups that had been observed during baseline measurements was no longer present in the second measurement. In another study, aging was shown to attenuate the vascular relaxation response to ACh in WKY (94). Thus, we might conclude that in the present study aging of the WKY group already started to attenuate the endothelium dependent microvascular response to ACh during the second assessment of skin microvascular reactivity. Taken together we propose that Vertigoheel® was not able to reverse the skin microvascular dysfunction that had already been present during baseline measurements in SHR, nor was it able to prevent the aging related development of endothelial dysfunction in WKY. However, skin perfusion response to the endothelium independent vasodilator SNP was stronger in Vertigoheel® treated WKY-V than in

untreated WKY-C. This suggests that aging related deterioration of vascular smooth muscle function in WKY was prevented or at least delayed by Vertigoheel® treatment.

5.2.2 Cerebral Microvascular Reactivity Assessment

Cerebral microvascular perfusion showed no significant difference among groups at baseline during normocapnic ventilation. Mild hypercapnia induced a marked perfusion increase in all groups. Increase in cerebral microvascular perfusion occurred about 15 minutes after onset of mild hypercapnia. Interestingly, the vasodilatory response was significantly greater in the SHR-V group than in SHR-C ($p < 0, 05$). The vasodilatory response to mild hypercapnia in SHR-V was not significantly different from that in WKY-V and WKY-C. On the other hand, the vasodilatory response was smaller in SHR-C compared to WKY-V and WKY-C. This is consistent with previous angiographic and MRI studies which have demonstrated a reduced cerebrovascular response to hypercapnia in SHR (95). Taken together with the present findings, we conclude that Vertigoheel® administration for 8 weeks restored the ameliorated cerebrovascular reactivity in SHR-V to the same level as in healthy WKY. This finding is also consistent with previous studies that have demonstrated a vasorelaxant effect and increased perfusion after Vertigoheel® administration isolated arteries and in humans, respectively (21;22).

5.2.3 Western blot and ELISA

To determine the mechanisms involved in the improvement of cerebral microvascular perfusion by Vertigoheel® in SHR, we also performed biochemical analysis: Western blotting and enzymatic assays with ELISA. A previous study showed that Vertigoheel® can induce vasorelaxation in isolated rat carotid arteries. This was associated with increased activities of adenylate and guanylate cyclases. In addition, administration of Vertigoheel® increased NO production in cultured endothelial cells (22). These results indicate that Vertigoheel® induces vasodilation involving endothelium mediated mechanisms, namely the NO/cGMP and the PGI_2/cAMP pathways. We tried to assess involvement of these pathways in the Vertigoheel® induced improvement of cerebral microvascular reactivity by assessing eNOS, PDE5, and PDE4 expression with Western blot and cAMP and cGMP tissue concentrations with ELISA.

5.2.3.1 eNOS

In Western blot assessment, eNOS expression was significantly higher in SHR-V compared with SHR-C, but similar to that in both, WKY-V and WKY-C. Also, eNOS expression was lower in SHR-C than in WKY-C. This finding is in line with previous studies that showed lower expression of eNOS in cerebral microvessels of SHR compared to WKY rats (96). In addition, exaggerated production of the superoxide anion ($\bullet O_2^-$) in the SHR vasculature has been demonstrated. NO can be scavenged by $\bullet O_2^-$ to form peroxynitrite which reduces the bioavailability of endothelium derived NO. Thus, diminished NO has been linked to decreased eNOS expression and increased $\bullet O2^-$ in hypertension and may lead to arterial dysfunction (97). After 8 weeks of Vertigoheel® treatment, eNOS expression in SHR-V was normalised to the level of healthy WKY rats. This finding suggests that eNOS was either up-regulated in SHR by Vertigoheel® treatment or Vertigoheel® prevented downregulation of eNOS during the treatment period. *Anamirta cocculus* and *Conium maculatum* are two ingredients of Vertigoheel® that have been shown to have antioxidant effects (98). Previous studies have shown that antioxidant therapy has beneficial effects on endothelial function. Thus, application of vitamin C and E, which are well known to have antioxidant effects, improved endothelial function in essential hypertension, hyperlipidemia, and coronary heart disease patients (99-101). The underlying mechanism may be scavenging of ROS by the antioxidants which would increase bioavailability of NO (102). Increased NO bioavailability is associated with increased eNOS expression and overall improvement of endothelial function (103).

In this study, vasodilation in the cerebral microvasculature was induced by hypercapnia. Hypercapnia is one of the most potent vasodilating stimuli in the cerebral circulation of mammals. Several in vivo studies have suggested that vasodilation in response to increased pCO_2 may be mediated, at least in part, by NO (104-106). Animal experiment studies have suggested that in the brain NO can be produced by endothelial cells, astrocytes and neurons (38). These cells form the components of the neurovascular unit that controls cerebrovascular metabolic regulation (107). Cerebrovascular reactivity in response to CO_2 is impaired in diabetic or hypertensive patients with endothelial dysfunction (104), suggesting an important role for endothelial cells in modulating the CBF response to CO_2 (107). In experimental animals, light/dye endothelial injury inhibited the hypercapnia induced cerebrovascular dilatation in anesthetized juvenile pigs, which was additionally sensitive to the eNOS inhibitor L-NAME and to soluble guanylate cyclase inhibition, indicating that endothelial NO may participate significantly in the hypercapnia induced vasodilatation (38). Based on these findings we propose

that the stronger hypercapnia induced cerebral microvascular vasodilatory response in SHR-V compared to SHR-C might be related to increase NO bioavailability and eNOS expression in SHR-V, possibly mediated by antioxidant properties of Vertigoheel®. This conclusion is consistent with observations of increased eNOS expression in SHR after antioxidant treatment (97;108). One of the ingredients of Vertigoheel, *Anamirta cocculus*, has also been shown to have antioxidant effect *in vivo* (109). Moreover, *Anamirta cocculus* contains quartenary alkaloids such as berberine (98;110), palmatine (111), or magnoflorine (112) which have also been shown to have antioxidant properties. Taken together, the present findings demonstrate that Vertigoheel® increases eNOS expression in SHR which might be mediated by antioxidant properties of Vertigoheel®.

5.2.3.2 PDE5

The NO-cGMP vasodilatory pathway in vascular smooth muscle cells involves PDE5. PDE5 participates in smooth muscle tone regulation by selectively hydrolysing the second messenger cGMP to inactive GMP (65). PDE5 inhibition has been shown to enhance the vasodilatory effect of NO (113). The present results show that the increased eNOS expression in SHR-V was not associated with a significant alteration in PDE5 expression. The expression of PDE5 showed no significant difference in SHR-V compared with SHR-C. There was also no significant difference of PDE5 expression between the WKY-V and WKY-C groups. This finding is in contrast with a previous *in vitro* study that has observed an inhibitory effect of *Conium maculatum,* one ingredient of Vertigoheel®, on PDE5 expression (22). This discrepancy might be explained by the higher dosage used in the previous *in vitro* study.

5.2.3.3 PDE4

Another mechanism involved in hypercapnia induced cerebral vascular vasodilation is mediated by the PGI_2/cAMP pathway (52). In vascular smooth muscle cells PDE4 specifically degrades the second messenger cAMP to inactive AMP (7;114). PDE4 inhibition has been shown to increase intracellular cAMP levels and induce vasodilation (115). However, in our study we found that Vertigoheel® has no effect on PDE4. There is no significant difference on PDE4 expression either between SHR-V and SHR-C group or WKY-V and WKY-C group.

5.2.3.4 cAMP and cGMP

In several vasodilatory signalling pathways cAMP and cGMP act as second messengers to mediate relaxation in vascular smooth muscle cells (116). cAMP is synthesized from adenosine triphosphate (ATP) by adenylate cyclase (30;38;50;55) and cGMP is synthesized from guanosine triphosphate (GTP) by guanylate cyclase (59). The concentrations of cAMP and cGMP in smooth muscle cells are controlled not only by the synthesis rates but also by their degradation by phosphodiesterases. Some phosphodiesterases can degrade both, cAMP and cGMP but PDE4 specifically degrades cAMP, while PDE5 is specific for cGMP (30). Previous *in vitro* study showed that Vertigoheel® stimulated adenylate cyclase activity which was replicated with corresponding concentrations of its ingredient *Anamirta cocculus.* In addition, the Vertigoheel® ingredient *Conium maculatum* dose dependently inhibited PDE5 activity (22). While we observed significant differences of eNOS expression between SHR-V and SHR-C, this is not associated with corresponding differences in cGMP concentrations. This is also reflected by the lack of significant correlations of cGMP with the enzyme expressions. The reasons for this discrepancy remain unknown. We can only speculate that in the case of cGMP, endothelial eNOS activity is also regulated by posttranslational mechanisms which are not reflected by protein expression. Also, the cGMP concentrations were very low, often close to the limit of detection of the ELISA test kit. According to general experience measurement errors may be particularly large in this low concentration range.

6. Conclusion

In conclusion, we demonstrated that Vertigoheel® can increase cerebral microvascular perfusion in SHR. We propose that the mechanisms involved in this effect are associated with increased eNOS expression. Further studies should aim at investigating the putative antioxidant mechanisms of Vertigoheel® such as effects on NADPH or ROS activities, or on histological assessment of the cerebral microvasculature to study microvascular remodelling.

7 Reference List

(1) Lunenfeld B, Stratton P. The clinical consequences of an ageing world and preventive strategies. Best Pract Res Clin Obstet Gynaecol 2013 Oct;27(5):643-59.

(2) United Nations Departement of Economic and Social Affairs Population Division. World Population Ageing 2009. http://www.un.org/esa/population/publications/WPA2009/WPA2009_WorkingPaper.pdf (accessed August 1, 2014)

(3) Duron E, Hanon O. Hypertension, cognitive decline and dementia. Arch Cardiovasc Dis 2008 Mar;101(3):181-9.

(4) Alzheimer Disease International. Alzheimer Disease International. World Alzheimer Report 2010: The global economic impact of dementia. 2010. https://www.alz.co.uk/research/files/WorldAlzheimerReport2010.pdf (accessed August 18, 2014)

(5) Wimo A, Jonsson L, Bond J, Prince M, Winblad B. The worldwide economic impact of dementia 2010. Alzheimers Dement 2013 Jan;9(1):1-11.

(6) Howard G, Goff DC. Population shifts and the future of stroke: forecasts of the future burden of stroke. Ann N Y Acad Sci 2012 Sep;1268:14-20.

(7) Roman GC. Vascular dementia. Advances in nosology, diagnosis, treatment and prevention. Panminerva Med 2004 Dec;46(4):207-15.

(8) Baskys A, Hou AC. Vascular dementia: pharmacological treatment approaches and perspectives. Clin Interv Aging 2007;2(3):327-35.

(9) Williams PS, Rands G, Orrel M, Spector A. Aspirin for vascular dementia. Cochrane Database Syst Rev 2000;(4):CD001296.

(10) Ritter A, Pillai JA. Treatment of Vascular Cognitive Impairment. Curr Treat Options Neurol 2015 Aug;17(8):367.

(11) Okamoto K, Tanaka M, Kondo S. Treatment of vascular dementia. Ann N Y Acad Sci 2002 Nov;977:507-12.

(12) Tadic M, Cuspidi C, Hering D. Hypertension and cognitive dysfunction in elderly: blood pressure management for this global burden. BMC Cardiovasc Disord 2016 Nov 3;16(1):208.

(13) Kavirajan H, Schneider LS. Efficacy and adverse effects of cholinesterase inhibitors and memantine in vascular dementia: a meta-analysis of randomised controlled trials. Lancet Neurol 2007 Sep;6(9):782-92.

(14) Wehling M, Groth H. Challenges of longevity in developed countries: vascular prevention of dementia as an immediate clue to tackle an upcoming medical, social and economic stretch. Neurodegener Dis 2011;8(5):275-82.

(15) Róman GC. Clinical forms of vascular dementia. In: Paul RH, Cohen R, Ott BR, Slloway S, editors. Vascular dementia: Cerebrovascular mechanisms and clinical management.Totowa, New Jersey: Humana Press; 2005. p. 7-21.

(16) Vicario A, Del SM, Fernandez RA, Enders J, Zilberman J, Cerezo GH. Cognition and vascular risk factors: an epidemiological study. Int J Hypertens 2012;2012:783696.

(17) Cohen RA. Hypertension and cerebral blood flow: implications for the development of vascular cognitive impairment in the elderly. Stroke 2007 Jun;38(6):1715-7.

(18) O'Rourke MF, Safar ME. Relationship between aortic stiffening and microvascular disease in brain and kidney: cause and logic of therapy. Hypertension 2005 Jul;46(1):200-4.

(19) Weiser M, Strosser W, Klein P. Homeopathic vs conventional treatment of vertigo: a randomized double-blind controlled clinical study. Arch Otolaryngol Head Neck Surg 1998 Aug;124(8):879-85.

(20) Millikan CH, Futrell N. Vertigo of vascular origin. Arch Neurol 1990 Jan;47(1):12-3.

(21) Klopp R, Niemer W, Weiser M. Microcirculatory effects of a homeopathic preparation in patients with mild vertigo: an intravital microscopic study. Microvasc Res 2005 Jan;69(1-2):10-6.

(22) Heinle H, Tober C, Zhang D, Jaggi R, Kuebler WM. The low-dose combination preparation Vertigoheel activates cyclic nucleotide pathways and stimulates vasorelaxation. Clin Hemorheol Microcirc 2010;46(1):23-35.

(23) Levy BI, Ambrosio G, Pries AR, Struijker-Boudier HA. Microcirculation in hypertension: a new target for treatment? Circulation 2001 Aug 7;104(6):735-40.

(24) Amenta F, Tomassoni D. Spontaneously Hypertensive Rats (SHR): An animal model of vascular brain disorder. In: De Deyn PP, Van Dam D, editors. Animal Models of Dementia. Humana Press; 2011. p. 577-611.

(25) Roman GC. Vascular dementia revisited: diagnosis, pathogenesis, treatment, and prevention. Med Clin North Am 2002 May;86(3):477-99.

(26) Gorelick PB. Risk factors for vascular dementia and Alzheimer disease. Stroke 2004 Nov;35(11 Suppl 1):2620-2.

(27) Staekenborg SS, van Straaten EC, van der Flier WM, Lane R, Barkhof F, Scheltens P. Small vessel versus large vessel vascular dementia: risk factors and MRI findings. J Neurol 2008 Nov;255(11):1644-51.

(28) Roman GC, Erkinjuntti T, Wallin A, Pantoni L, Chui HC. Subcortical ischaemic vascular dementia. Lancet Neurol 2002 Nov;1(7):426-36.

(29) Schuff N, Matsumoto S, Kmiecik J, Studholme C, Du A, Ezekiel F, et al. Cerebral blood flow in ischemic vascular dementia and Alzheimer's disease, measured by arterial spin-labeling magnetic resonance imaging. Alzheimers Dement 2009 Nov;5(6):454-62.

(30) Iadecola C, Davisson RL. Hypertension and cerebrovascular dysfunction. Cell Metab 2008 Jun;7(6):476-84.

(31) Manolio TA, Olson J, Longstreth WT. Hypertension and cognitive function: pathophysiologic effects of hypertension on the brain. Curr Hypertens Rep 2003 Jun;5(3):255-61.

(32) Gorelick PB, Scuteri A, Black SE, Decarli C, Greenberg SM, Iadecola C, et al. Vascular contributions to cognitive impairment and dementia: a statement for healthcare professionals from the american heart association/american stroke association. Stroke 2011 Sep;42(9):2672-713.

(33) Selnes OA, Vinters HV. Vascular cognitive impairment. Nat Clin Pract Neurol 2006 Oct;2(10):538-47.

(34) Brown WR, Moody DM, Thore CR, Challa VR, Anstrom JA. Vascular dementia in leukoaraiosis may be a consequence of capillary loss not only in the lesions, but in normal-appearing white matter and cortex as well. J Neurol Sci 2007 Jun 15;257(1-2):62-6.

(35) Popescu BO, Toescu EC, Popescu LM, Bajenaru O, Muresanu DF, Schultzberg M, et al. Blood-brain barrier alterations in ageing and dementia. J Neurol Sci 2009 Aug 15;283(1-2):99-106.

(36) Farrall AJ, Wardlaw JM. Blood-brain barrier: ageing and microvascular disease--systematic review and meta-analysis. Neurobiol Aging 2009 Mar;30(3):337-52.

(37) Schreiber S, Bueche CZ, Garz C, Braun H. Blood brain barrier breakdown as the starting point of cerebral small vessel disease? - New insights from a rat model. Exp Transl Stroke Med 2013;5(1):4.

(38) Toda N, Ayajiki K, Okamura T. Cerebral blood flow regulation by nitric oxide: recent advances. Pharmacol Rev 2009 Mar;61(1):62-97.

(39) Tousoulis D, Kampoli AM, Tentolouris C, Papageorgiou N, Stefanadis C. The role of nitric oxide on endothelial function. Curr Vasc Pharmacol 2012 Jan;10(1):4-18.

(40) Schulz E, Gori T, Munzel T. Oxidative stress and endothelial dysfunction in hypertension. Hypertens Res 2011 Jun;34(6):665-73.

(41) Bennett S, Grant MM, Aldred S. Oxidative stress in vascular dementia and Alzheimer's disease: a common pathology. J Alzheimers Dis 2009;17(2):245-57.

(42) Morillo GA, Abreu MF. Ultrastructural characterization of small vessel disease in skin biopsies in vascular cognitive impairment type subcortical small-vessel ischemic disease. Preliminaries result towards pathophysiology and theurpaeutics aspects. In: Thompson R, editor. Microcirculation: Function, malfunction and measurement. New York: Nova Biomedical Books; 2009. p. 95-111.

(43) Tyagi A, Sethi AK, Girotra G, Mohta M. The microcirculation in sepsis. Indian J Anaesth 2009 Jun;53(3):281-93.

(44) Iadecola C, Nedergaard M. Glial regulation of the cerebral microvasculature. Nat Neurosci 2007 Nov;10(11):1369-76.

(45) Bell RD, Zlokovic BV. Neurovascular mechanisms and blood-brain barrier disorder in Alzheimer's disease. Acta Neuropathol 2009 Jul;118(1):103-13.

(46) Chow N, Bell RD, Deane R, Streb JW, Chen J, Brooks A, et al. Serum response factor and myocardin mediate arterial hypercontractility and cerebral blood flow dysregulation in Alzheimer's phenotype. Proc Natl Acad Sci U S A 2007 Jan 16;104(3):823-8.

(47) Iadecola C. Neurovascular regulation in the normal brain and in Alzheimer's disease. Nat Rev Neurosci 2004 May;5(5):347-60.

(48) Iadecola C. The overlap between neurodegenerative and vascular factors in the pathogenesis of dementia. Acta Neuropathol 2010 Sep;120(3):287-96.

(49) Ballabh P, Braun A, Nedergaard M. The blood-brain barrier: an overview: structure, regulation, and clinical implications. Neurobiol Dis 2004 Jun;16(1):1-13.

(50) Tuma RF. The cerebral microcirculation. In: Tuma RF, Duran WN, Ley K, editors. Handbook of physiology and microcirculation. Academic Press; 2013. p. 485-520.

(51) Kuhnline Sloan CD, Nandi P, Linz TH, Aldrich JV, Audus KL, Lunte SM. Analytical and biological methods for probing the blood-brain barrier. Annu Rev Anal Chem (Palo Alto Calif) 2012;5:505-31.

(52) Abbott NJ, Ronnback L, Hansson E. Astrocyte-endothelial interactions at the blood-brain barrier. Nat Rev Neurosci 2006 Jan;7(1):41-53.

(53) Hawkins RA, O'Kane RL, Simpson IA, Vina JR. Structure of the blood-brain barrier and its role in the transport of amino acids. J Nutr 2006 Jan;136(1 Suppl):218S-26S.

(54) Hawkins BT, Davis TP. The blood-brain barrier/neurovascular unit in health and disease. Pharmacol Rev 2005 Jun;57(2):173-85.

(55) Peterson EC, Wang Z, Britz G. Regulation of cerebral blood flow. Int J Vasc Med 2011;2011:823525.

(56) Novak V, Yang AC, Lepicovsky L, Goldberger AL, Lipsitz LA, Peng CK. Multimodal pressure-flow method to assess dynamics of cerebral autoregulation in stroke and hypertension. Biomed Eng Online 2004 Oct 25;3(1):39.

(57) ter LM, van Dijk JM, Elting JW, Staal MJ, Absalom AR. Sympathetic regulation of cerebral blood flow in humans: a review. Br J Anaesth 2013 Sep;111(3):361-7.

(58) Koehler RC, Gebremedhin D, Harder DR. Role of astrocytes in cerebrovascular regulation. J Appl Physiol (1985) 2006 Jan;100(1):307-17.

(59) Negash S, Gao Y, Zhou W, Liu J, Chinta S, Raj JU. Regulation of cGMP-dependent protein kinase-mediated vasodilation by hypoxia-induced reactive species in ovine fetal pulmonary veins. Am J Physiol Lung Cell Mol Physiol 2007 Oct;293(4):L1012-L1020.

(60) Duchemin S, Boily M, Sadekova N, Girouard H. The complex contribution of NOS interneurons in the physiology of cerebrovascular regulation. Front Neural Circuits 2012;6:51.

(61) Bomboi G, Castello L, Cosentino F, Giubilei F, Orzi F, Volpe M. Alzheimer's disease and endothelial dysfunction. Neurol Sci 2010 Feb;31(1):1-8.

(62) Mitchell JA, Ali F, Bailey L, Moreno L, Harrington LS. Role of nitric oxide and prostacyclin as vasoactive hormones released by the endothelium. Exp Physiol 2008 Jan;93(1):141-7.

(63) Andresen J, Shafi NI, Bryan RM, Jr. Endothelial influences on cerebrovascular tone. J Appl Physiol (1985) 2006 Jan;100(1):318-27.

(64) Tsai EJ, Kass DA. Cyclic GMP signaling in cardiovascular pathophysiology and therapeutics. Pharmacol Ther 2009 Jun;122(3):216-38.

(65) Kass DA, Champion HC, Beavo JA. Phosphodiesterase type 5: expanding roles in cardiovascular regulation. Circ Res 2007 Nov 26;101(11):1084-95.

(66) Okamoto K, AOKI K. Development of a strain of spontaneously hypertensive rats. Jpn Circ J 1963 Mar;27:282-93.

(67) Howells DW, Porritt MJ, Rewell SS, O'Collins V, Sena ES, van der Worp HB, et al. Different strokes for different folks: the rich diversity of animal models of focal cerebral ischemia. J Cereb Blood Flow Metab 2010 Aug;30(8):1412-31.

(68) Gianaros PJ, Greer PJ, Ryan CM, Jennings JR. Higher blood pressure predicts lower regional grey matter volume: Consequences on short-term information processing. Neuroimage 2006 Jun;31(2):754-65.

(69) Paiardi S, Rodella LF, De CC, Porteri E, Boari GE, Rezzani R, et al. Immunohistochemical evaluation of microvascular rarefaction in hypertensive humans and in spontaneously hypertensive rats. Clin Hemorheol Microcirc 2009;42(4):259-68.

(70) Chillon JM, Baumbach GL. Effects of indapamide, a thiazide-like diuretic, on structure of cerebral arterioles in hypertensive rats. Hypertension 2004 May;43(5):1092-7.

(71) Schneider B, Klein P, Weiser M. Treatment of vertigo with a homeopathic complex remedy compared with usual treatments: a meta-analysis of clinical trials. Arzneimittelforschung 2005;55(1):23-9.

(72) Issing W, Klein P, Weiser M. The homeopathic preparation Vertigoheel versus Ginkgo biloba in the treatment of vertigo in an elderly population: a double-blinded, randomized, controlled clinical trial. J Altern Complement Med 2005 Feb;11(1):155-60.

(73) Grad A, Baloh RW. Vertigo of vascular origin. Clinical and electronystagmographic features in 84 cases. Arch Neurol 1989 Mar;46(3):281-4.

(74) Nakase H, Kempski OS, Heimann A, Takeshima T, Tintera J. Microcirculation after cerebral venous occlusions as assessed by laser Doppler scanning. J Neurosurg 1997 Aug;87(2):307-14.

(75) Kerem A, Yin J, Kaestle SM, Hoffmann J, Schoene AM, Singh B, et al. Lung endothelial dysfunction in congestive heart failure: role of impaired Ca2+ signaling and cytoskeletal reorganization. Circ Res 2010 Apr 2;106(6):1103-16.

(76) Mordi I, Mordi N, Delles C, Tzemos N. Endothelial dysfunction in human essential hypertension. J Hypertens 2016 Aug;34(8):1464-72.

(77) Farkas K, Kolossvary E, Jarai Z, Nemcsik J, Farsang C. Non-invasive assessment of microvascular endothelial function by laser Doppler flowmetry in patients with essential hypertension. Atherosclerosis 2004 Mar;173(1):97-102.

(78) Thuillez C, Richard V. Targeting endothelial dysfunction in hypertensive subjects. J Hum Hypertens 2005 Jun;19 Suppl 1:S21-S25.

(79) Potenza MA, Marasciulo FL, Tarquinio M, Quon MJ, Montagnani M. Treatment of spontaneously hypertensive rats with rosiglitazone and/or enalapril restores balance between vasodilator and vasoconstrictor actions of insulin with simultaneous improvement in hypertension and insulin resistance. Diabetes 2006 Dec;55(12):3594-603.

(80) Orekhova LY, Barmasheva AA. Doppler flowmetry as a tool of predictive, preventive and personalised dentistry. EPMA J 2013;4(1):21.

(81) Yvonne-Tee GB, Rasool AH, Halim AS, Rahman AR. Noninvasive assessment of cutaneous vascular function in vivo using capillaroscopy, plethysmography and laser-Doppler instruments: its strengths and weaknesses. Clin Hemorheol Microcirc 2006;34(4):457-73.

(82) Shiogai Y, Stefanovska A, McClintock PV. Nonlinear dynamics of cardiovascular ageing. Phys Rep 2010 Mar;488(2-3):51-110.

(83) Jiwa NS, Garrad P, Hainsworth AH. Experimental models of vascular dementia and vascular cognitive impairment: a systematic review. Journal of Neurochemistry 2010;115:814-28.

(84) Tayebati SK, Tomassoni D, Amenta F. Spontaneously hypertensive rat as a model of vascular brain disorder: Microanatomy, neurochemistry and behavior. Journal of the Neurological Sciences 2012;322:241-9.

(85) Murfee WL, Schmid-Schönbein GW. Chapter 12. Structure of microvascular networks in genetic hypertension. Methods in Enzymology 2015;444:271-84.

(86) Rush JW, Quadrilatero J, Levy AS, Ford RJ. Chronic resveratrol enhances endothelium-dependent relaxation but does not alter eNOS levels in aorta of spontaneously hypertensive rats. Exp Biol Med (Maywood) 2007 Jun;232(6):814-22.

(87) Mori Y, Ohyanagi M, Koida S, Ueda A, Ishiko K, Iwasaki T. Effects of endothelium-derived hyperpolarizing factor and nitric oxide on endothelial function in femoral

resistance arteries of spontaneously hypertensive rats. Hypertens Res 2006 Mar;29(3):187-95.

(88) Kubota Y, Tanaka N, Kagota S, Nakamura K, Kunitomo M, Umegaki K, et al. Effects of Ginkgo biloba extract on blood pressure and vascular endothelial response by acetylcholine in spontaneously hypertensive rats. J Pharm Pharmacol 2006 Feb;58(2):243-9.

(89) Suzuki A, Yamamoto M, Jokura H, Fujii A, Tokimitsu I, Hase T, et al. Ferulic acid restores endothelium-dependent vasodilation in aortas of spontaneously hypertensive rats. Am J Hypertens 2007 May;20(5):508-13.

(90) Orescanin ZS, Milovanovic SR, Spasic SD, Jones DR, Spasic MB. Different responses of mesenteric artery from normotensive and spontaneously hypertensive rats to nitric oxide and its redox congeners. Pharmacol Rep 2007 May;59(3):315-22.

(91) Orescanin Z, Milovanovic SR. Effect of L-arginine on the relaxation caused by sodium nitroprusside on isolated rat renal artery. Acta Physiol Hung 2006 Dec;93(4):271-83.

(92) Yamamoto M, Suzuki A, Jokura H, Yamamoto N, Hase T. Glucosyl hesperidin prevents endothelial dysfunction and oxidative stress in spontaneously hypertensive rats. Nutrition 2008 May;24(5):470-6.

(93) Somoza B, Abderrahim F, Gonzalez JM, Conde MV, Arribas SM, Starcher B, et al. Short-term treatment of spontaneously hypertensive rats with liver growth factor reduces carotid artery fibrosis, improves vascular function, and lowers blood pressure. Cardiovasc Res 2006 Feb 15;69(3):764-71.

(94) Imaoka Y, Osanai T, Kamada T, Mio Y, Satoh K, Okumura K. Nitric oxide-dependent vasodilator mechanism is not impaired by hypertension but is diminished with aging in the rat aorta. J Cardiovasc Pharmacol 1999 May;33(5):756-61.

(95) Nakajima S, Kondoh T, Morishita A, Yamashita H, Kohmura E, Sakurai T, et al. Loss of CO2-induced distensibility in cerebral arteries with chronic hypertension or vasospasm after subarachnoid hemorrhage. Kobe J Med Sci 2007;53(6):317-26.

(96) Yamakawa H, Jezova M, Ando H, Saavedra JM. Normalization of endothelial and inducible nitric oxide synthase expression in brain microvessels of spontaneously hypertensive rats by angiotensin II AT1 receptor inhibition. J Cereb Blood Flow Metab 2003 Mar;23(3):371-80.

(97) Zhang JX, Yang JR, Chen GX, Tang LJ, Li WX, Yang H, et al. Sesamin ameliorates arterial dysfunction in spontaneously hypertensive rats via downregulation of NADPH oxidase subunits and upregulation of eNOS expression. Acta Pharmacol Sin 2013 Jul;34(7):912-20.

(98) Abd El-Wahab AE, Ghareeb DA, Sarhan EE, Abu-Serie MM, El Demellawy MA. In vitro biological assessment of Berberis vulgaris and its active constituent, berberine: antioxidants, anti-acetylcholinesterase, anti-diabetic and anticancer effects. BMC Complement Altern Med 2013;13:218.

(99) Grassi D, Desideri G, Ferri C. Flavanoids: antioxidants against atherosclerosis. Nutrients 2010 Aug;2(8):889-902.

(100) Plantinga Y, Ghiadoni L, Magagna A, Giannarelli C, Franzoni F, Taddei S, et al. Supplementation with vitamins C and E improves arterial stiffness and endothelial function in essential hypertensive patients. Am J Hypertens 2007 Apr;20(4):392-7.

(101) Engler MM, Engler MB, Malloy MJ, Chiu EY, Schloetter MC, Paul SM, et al. Antioxidant vitamins C and E improve endothelial function in children with hyperlipidemia: Endothelial Assessment of Risk from Lipids in Youth (EARLY) Trial. Circulation 2003 Sep 2;108(9):1059-63.

(102) Wang W, Jittikanont S, Falk SA, Li P, Feng L, Gengaro PE, et al. Interaction among nitric oxide, reactive oxygen species, and antioxidants during endotoxemia-related acute renal failure. Am J Physiol Renal Physiol 2003 Mar;284(3):F532-F537.

(103) Rimoldi SF, Sartori C, Rexhaj E, Bailey DM, Marchi SF, McEneny J, et al. Antioxidants improve vascular function in children conceived by assisted reproductive technologies: A randomized double-blind placebo-controlled trial. Eur J Prev Cardiol 2014 May 9.

(104) Lavi S, Gaitini D, Milloul V, Jacob G. Impaired cerebral CO2 vasoreactivity: association with endothelial dysfunction. Am J Physiol Heart Circ Physiol 2006 Oct;291(4):H1856-H1861.

(105) Yoon S, Zuccarello M, Rapoport RM. pCO(2) and pH regulation of cerebral blood flow. Front Physiol 2012;3:365.

(106) Brian JE, Jr. Carbon dioxide and the cerebral circulation. Anesthesiology 1998 May;88(5):1365-86.

(107) Fathi AR, Yang C, Bakhtian KD, Qi M, Lonser RR, Pluta RM. Carbon dioxide influence on nitric oxide production in endothelial cells and astrocytes: cellular mechanisms. Brain Res 2011 Apr 22;1386:50-7.

(108) Sanchez M, Galisteo M, Vera R, Villar IC, Zarzuelo A, Tamargo J, et al. Quercetin downregulates NADPH oxidase, increases eNOS activity and prevents endothelial dysfunction in spontaneously hypertensive rats. J Hypertens 2006 Jan;24(1):75-84.

(109) Palasuwan A, Soogarun S, Lertlum T, Pradniwat P, Wiwanitkit V. Inhibition of Heinz body induction in an in vitro model and total antioxidant activity of medicinal Thai plants. Asian Pac J Cancer Prev 2005 Oct;6(4):458-63.

(110) Bhutada P, Mundhada Y, Bansod K, Tawari S, Patil S, Dixit P, et al. Protection of cholinergic and antioxidant system contributes to the effect of berberine ameliorating memory dysfunction in rat model of streptozotocin-induced diabetes. Behav Brain Res 2011 Jun 20;220(1):30-41.

(111) Dhingra D, Kumar V. Memory-enhancing activity of palmatine in mice using elevated plus maze and morris water maze. Adv Pharmacol Sci 2012;2012:357368.

(112) Hung TM, Na M, Min BS, Zhang X, Lee I, Ngoc TM, et al. Protective effect of magnoflorine isolated from coptidis rhizoma on Cu2+-induced oxidation of human low density lipoprotein. Planta Med 2007 Oct;73(12):1281-4.

(113) Yaguas K, Bautista R, Quiroz Y, Ferrebuz A, Pons H, Franco M, et al. Chronic sildenafil treatment corrects endothelial dysfunction and improves hypertension. Am J Nephrol 2010;31(4):283-91.

(114) Omori K, Kotera J. Overview of PDEs and their regulation. Circ Res 2007 Feb 16;100(3):309-27.

(115) Dagues N, Pawlowski V, Sobry C, Hanton G, Borde F, Soler S, et al. Investigation of the molecular mechanisms preceding PDE4 inhibitor-induced vasculopathy in rats: tissue inhibitor of metalloproteinase 1, a potential predictive biomarker. Toxicol Sci 2007 Nov;100(1):238-47.

(116) Francis SH, Busch JL, Corbin JD, Sibley D. cGMP-dependent protein kinases and cGMP phosphodiesterases in nitric oxide and cGMP action. Pharmacol Rev 2010 Sep;62(3):525-63.

8. Appendix

My curriculum vitae does not appear in the electronic version of my paper for reasons of data protection.

List of Publications

1. Klein N, Gembardt F, Supé S, Kaestle SM, Nickles H, **Erfinanda L**, Lei X, Yin J, Wang L, Mertens M, Szaszi K, Walther T, Kuebler WM. Angiotensin-(1-7) protects from experimental acute lung injury. Crit Care Med 2013 Nov;41(11):334-43
2. Yin J, Michalick L, Tang C, Tabuchi A, Goldenberg N, Dan Q, Awwad K, Wang L, **Erfinanda L**, Nouailles G, Witzenrath M, Vogelzang A, Lv L, Lee WL, Zhang H, Rotstein O, Kapus A, Szaszi K, Fleming I, Liedtke WB, Kuppe H, Kuebler WM. Role of Transient Receptor Potential Vanilloid 4 in Neutrophil Activation and Acute Lung Injury. Am J Respir Cell Mol Biol. 2016 Mar;54(3):370-83
3. Michalick L, **Erfinanda L**, Weichelt U, van der Giet M, Liedtke W, Kuebler WM. Transient Receptor Potential Vanilloid 4 and Serum Glucocorticoid-regulated Kinase 1 Are Critical Mediators of Lung Injury in Overventilated Mice in Vivo. Anesthesiology. 2016 Nov 18

Affidavit

"I, Lasti, Erfinanda, certify under penalty of perjury by my own signature that I have submitted the thesis on the topic "Effects of Vertigoheel® on the Microcirculation of Spontaneously Hypertensive Rats" I wrote this thesis independently and without assistance from third parties, I used no other aids than the listed sources and resources.

All points based literally or in spirit on publications or presentations of other authors are, as such, in proper citations (see "uniform requirements for manuscripts (URM)" the ICMJE www.icmje.org) indicated. The sections on methodology (in particular practical work, laboratory requirements, statistical processing) and results (in particular images, graphics and tables) correspond to the URM (s.o) and are answered by me. My interest in any publications to this dissertation corresponds to those that are specified in the following joint declaration with the responsible person and supervisor. All publications resulting from this thesis and which I am author correspond to the URM (see above) and I am solely responsible.

The importance of this affidavit and the criminal consequences of a false affidavit (section 156,161 of the Criminal Code) are known to me and I understand the rights and responsibilities stated therein.

Date Signature

Declaration of any eventual publications

1. Klein N, Gembardt F, Supé S, Kaestle SM, Nickles H, **Erfinanda L**, Lei X, Yin J, Wang L, Mertens M, Szaszi K, Walther T, Kuebler WM. Angiotensin-(1-7) protects from experimental acute lung injury. Crit Care Med 2013 Nov;41(11):334-43
   Contribution in detail: Contribute in *in vivo* experiment and histology analysis.
2. Yin J, Michalick L, Tang C, Tabuchi A, Goldenberg N, Dan Q, Awwad K, Wang L, **Erfinanda L**, Nouailles G, Witzenrath M, Vogelzang A, Lv L, Lee WL, Zhang H, Rotstein O, Kapus A, Szaszi K, Fleming I, Liedtke WB, Kuppe H, Kuebler WM. Role of Transient Receptor Potential Vanilloid 4 in Neutrophil Activation and Acute Lung Injury. Am J Respir Cell Mol Biol. 2016 Mar;54(3):370-83
   Contribution in detail: Contribute in *in vivo* experiment and biochemistry analysis.
3. Michalick L, **Erfinanda L**, Weichelt U, van der Giet M, Liedtke W, Kuebler WM. Transient Receptor Potential Vanilloid 4 and Serum Glucocorticoid-regulated Kinase 1 Are Critical Mediators of Lung Injury in Overventilated Mice in Vivo. Anesthesiology. 2017 Feb;126(2):300-311
   Contribution in detail: Contribute in biochemistry analysis.

Signature, date and stamp of the supervising University teacher

_____

Signature of the doctoral candidate

_____

Acknowledgement

My deepest gratitude goes first and foremost to Professor Helmut Habazettl, my supervisor, for his trust, constant encouragement and motivation. He has always guided and encouraged me through the process of this thesis which has taught me to trust myself and never lose faith in every situation. Without his support, this thesis could not have reached its present form.

I would like to thank the company Heel and Dr. Yvonne Burmeister from Heel for supporting this project. I want to thank Professor Axel Pries for allowing me to work in his lab. I would like to thank Professor Wolfgang Kübler and his group Dr.med.vet Rudi Samapati, Dr.rer.nat Julia Hoffmann, Hannah Nickles, Laura Michalick, Stefanie Supé, and Dr. Ulrike Weichelt for helping me through this project.

I would like to thank my colleagues and friends within the Institute of Physiology, Charité, Dr Bianca Nitzsche, Björn Hoffmann, Weronika Kuzyniak, Dr. Janine Berkholz and Dr. med. Alex Marki for help in work and life. Thanks to Mrs. Sylvia Plog for the excellent technical assistance. Thanks to our kind secretaries Mrs. Cornelia Marruhn, Mrs. Brigitte Bünsch, and Mrs Felicitas Kern.